Carbon in One Dimension: Structural Analysis of the Higher Conjugated Polyynes

Slawomir Szafert*,† and J. A. Gladysz*,‡

Department of Chemistry, University of Wroclaw, 14 F. Joliot-Curie, Wroclaw, Poland, and Institut für Organische Chemie, Friedrich-Alexander-Universität Erlangen-Nürnberg, Henkestrasse 42, 91054 Erlangen, Germany

Received May 21, 2003

Contents

1. Introduction

The previous decade has witnessed an ongoing series of stunning breakthroughs in carbon allotrope chemistry.[1,2] This field has attracted scientists from all disciplines, and is playing a leading role in the nanotechnology boom. However, the polymeric sp carbon allotrope, often termed "carbyne", remains an unsettled and somewhat controversial topic.[3] This substance ranks in conceptual importance as a full equal of diamond, the polymeric, three-dimensional sp^3 allotrope, and graphite, the polymeric, two-dimensional sp^2 allotrope. It should have a linear ground state, but remains difficult to generate, isolate, and characterize. All polymeric carbon allotropes must have some type of capping endgroup, and in this context carbyne has two limiting forms: one with dicoordinate terminal carbons (X−C≡) and consisting of alternating triple and single bonds, and another with tricoordinate terminal carbons (X_2C═) and consisting solely of double bonds.

In attempts to model carbyne and gain added insight, various series of oligoynes or polyynediyl systems X(C≡C)$_n$X have been synthesized and studied. There is an extensive older literature of such compounds, and a modern literature due largely to Gladysz[4,5] and Hirsch[6,7] that provides leading references to earlier work. These series have been used to define the effect of chain length upon various molecular properties. One would expect that they asymptotically approach those of the polyyne or triply/singly bonded form of carbyne. Note that any measurable quantity, such as an absorption band, NMR chemical shift or coupling constant, or redox

Slawomir Szafert received his Ph.D. degree in 1996 at the University of Wroclaw (Poland) under the supervision of Prof. P. Sobota. He was subsequently awarded a fellowship from the Fulbright Foundation for postdoctoral research. He then joined the research group of J. A. Gladysz at the University of Utah. In August of 1999, he returned to Wroclaw to take an adjunct position on the team of Prof. P. Sobota. His scientific interests are focused on the asymmetric synthesis and catalysis, as well as organometallic chemistry.

John A. Gladysz was educated at Western Michigan University, the University of Michigan, and Stanford University. His academic career has included faculty appointments at UCLA (1974–1982), the University of Utah (1982–1998), and the University of Erlangen-Nuremberg (1998-present). His honors include the ACS Award in Organometallic Chemistry (1994), and a von Humboldt Foundation Research Award for Senior Scientists (1995–96). He has been an Associate Editor of *Chemical Reviews* since 1984.

† University of Wroclaw.
‡ Friedrich-Alexander-Universität Erlangen-Nürnberg.

10.1021/cr030041o CCC: $44.00
Published on Web 10/29/2003

potential can be plotted against $1/n$, where n is the number of alkyne units. When well-defined relationships emerge, extrapolation to the y intercept ($1/n = 0$) should give the value for the corresponding $(C{\equiv}C)_\infty$ species. In principle, series of model cumulenes $X_2C{=}(C{=}C)_n{=}CX_2$ could similarly be analyzed. However, such compounds become unstable at much shorter chain lengths.[8]

The structure of carbyne is of interest from several standpoints. For example, as a polyyne is lengthened, will the triple and single bond lengths converge to one value, or approach two different values? The former (bond length equalization) implies a vanishing HOMO/LUMO energy gap. The latter (bond length alternation) implies a persistent energy gap, or from a solid-state physics perspective a Peierls distortion.[4−7] Another question is to what degree carbyne can easily bend. There has been conjecture that long sp carbon chains might distort, triggering isomerization to fullerenes or other carbon allotropes.[9−11] Although there are many conceivable experimental and computational[12] probes of these possibilities, crystallography represents an obvious approach.

In 1997, we analyzed all compounds with at least eight consecutive sp hybridized carbons that had been crystallographically characterized.[13] Six 1,3,5,7-tetraynes[9,13−17] and one 1,3,5,7,9-pentayne[18] were known at that time, but no comparable cumulenes. In the meantime, the structures of many additional tetraynes and pentaynes have been determined, and data have become available for still higher polyynes. Accordingly, a comprehensive, interpretive review of the structures and packing motifs of the ca. 45 compounds currently in the literature or in various databases is presented below. This is done in a format optimized for a "living review" that can be periodically updated on the web version of *Chemical Reviews*, in accord with new capabilities planned by the publisher. As the numbers of compounds in various categories reach critical masses and/or grow further, additional insights and conclusions are certain to emerge.

This review also has implications for the rapidly growing disciplines of crystal engineering and crystal structure prediction. Current developments in the first area,[19] the enormous challenge of the latter,[20] and the distinction between them,[19b] have been eloquently described elsewhere. It can be argued that to develop predictive algorithms for how complex molecules pack, one must begin with fundamental types of building blocks. In other words, a "bottom-up" approach is needed. An sp carbon chain provides the closest possible approximation to a one-dimensional molecular rod. Clearly, an understanding of how these rodlike conjugated polyynes pack is necessary before one can hope to model molecules with two-dimensional shapes and ultimately garden-variety real-world molecules.[21] As detailed below, many interesting, tangible relationships emerge. There are of course a variety of "thicker" molecules that are often referred to as rodlike (e.g., *p*-phenylene or staffane systems).[22] There are also scattered older analyses of packing motifs of such rodlike molecules.[23]

Chart 1. Crystallographically Characterized 1,3,5,7-Tetraynes with Non-Metal-Containing Endgroups

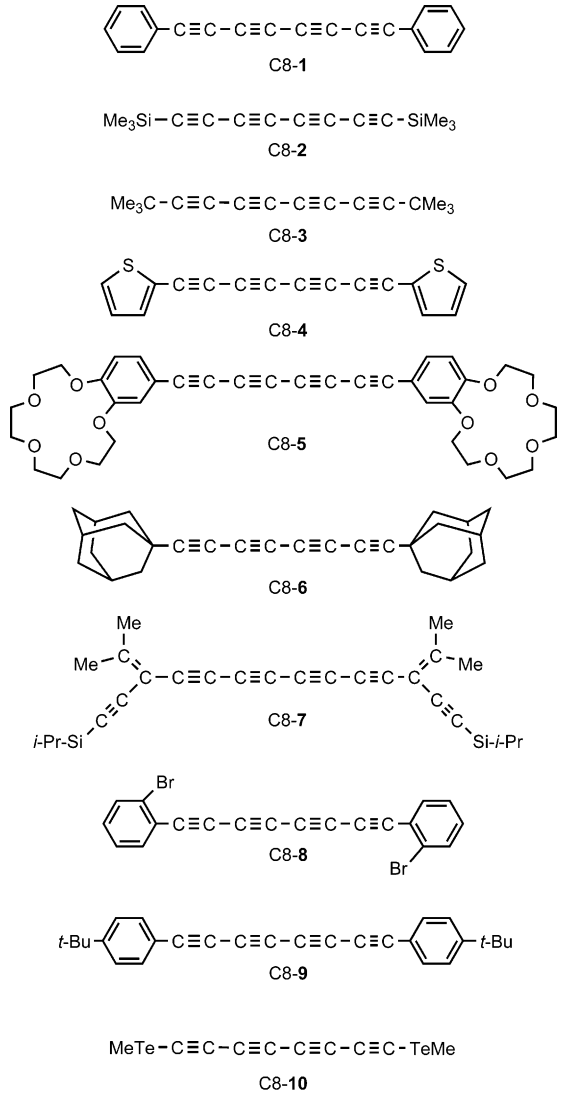

2. Classification of Polyynes

As a starting organizational point, all structurally characterized 1,3,5,7-tetraynes and higher homologues are illustrated in Charts 1−6. The numbering system utilized incorporates the sp carbon chain length. Chart 1 collects 1,3,5,7-tetraynes with non-metal-containing endgroups (C8-**1**−C8-**10**).[9,14,15,24−30] The sp chains in these molecules terminate with carbon−carbon, carbon−silicon, or carbon−tellurium bonds. Charts 2−4 collect 1,3,5,7-tetraynes with metal-containing endgroups.[4,13,16,17,29,31−38] Note that in Chart 2, some chains terminate with carbon−carbon bonds (C8-**12**-**13**, C8-**18**), and others with carbon-metal bonds (C8-**14**−**17**). Charts 3 and 4 depict monoplatinum (C8-**22**-**23**) and diplatinum (C8-**20**−**21**, C8-**24**−**27**, C8-**29**−**32**) complexes.[5,33−38] All examples in Chart 4 contain diphosphine ligands that bridge the two platinum atoms.

Chart 5 illustrates the two structurally characterized 1,3,5,7,9-pentaynes (C10-**1** and C10-**3**),[18,36] the second of which has a metal-containing endgroup, and the one 1,3,5,7,9,11-hexayne with non-metal-containing endgroups (C12-**1**).[29] Chart 6 collects

Chart 2. Crystallographically Characterized 1,3,5,7-Tetraynes with Metal-Containing Endgroups

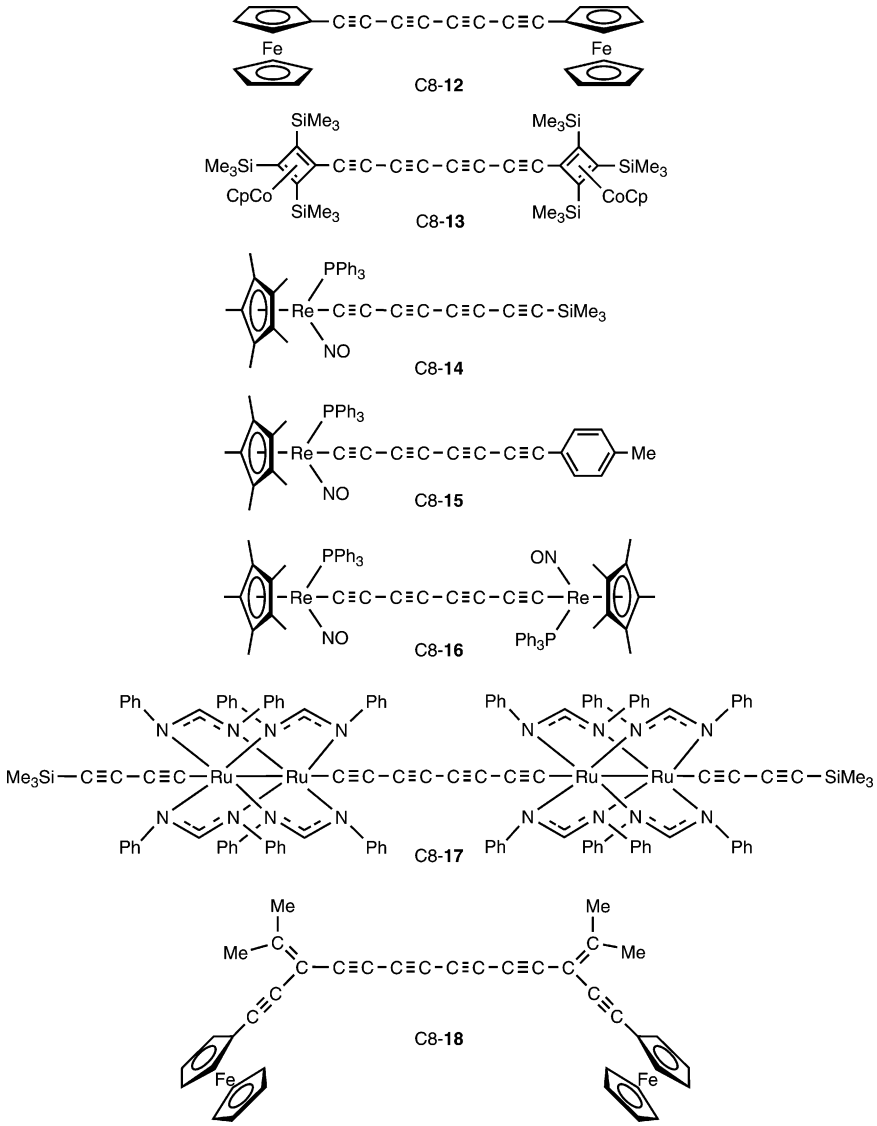

1,3,5,7,9,11-hexaynes with metal-containing endgroups (C12-**3**-**9**),[33,34,38−41] and the single example of a 1,3,5,7,9,11,13,15-octayne (C16-**1**).[34] Although the preceding groupings have arbitrary aspects, there are no obviously superior alternatives for analyzing the many phenomena below. When the terms tetrayne, pentayne, hexayne, and octayne are used, conjugated 1,3,5,7-, 1,3,5,7,9-, 1,3,5,7,9,11-, and 1,3,5,7,9,11,13,-15-systems are always implied. Note though that the 1,3,5,7-tetraynes C8-**7** and C8-**18** are in fact hexaynes, and C8-**17** and C8-**26** are in fact octaynes.

Compounds with even numbers of triple bonds (tetraynes, hexaynes, octaynes) greatly predominate in Charts 1−6. This does not reflect any innate proclivity toward crystallinity. Rather, most of these compounds are prepared by the oxidative homocoupling of terminal polyynes, which by necessity results in an even number of triple bonds, as well as identical endgroups. The only compounds with nonidentical endgroups are C8-**14**, C8-**15**, C8-**22**, C8-**23**, and C10-**3**. To systematize comparisons, the group with the higher Cahn−Ingold−Prelog priority is designated X, and the lower priority is designated X′.

For some compounds in Charts 1−6, more than one crystal structure is available. For example, C8-**1** and C8-**7** exhibit polymorphism.[14,27] Three modifications have been reported for the former, but unfortunately no atomic coordinates are available. The two modifications of the latter are designated C8-**7a** and C8-**7b**. For C8-**29**, C8-**31**, and C8-**32** two different solvates have been characterized.[38] Such solvates are often termed pseudopolymorphs.[42] In the case of C12-**9**, two independent molecules are found in the unit cell (designated C12-**9** and C12-**9′**), each with markedly different conformations.[38] In all of these cases, both forms are analyzed below. Finally, dumbbell-like C8-**6** (Chart 1) could be crystallized with various guests to give different inclusion compounds, but only one data set (C8-**6**·BU·C, formed from a mixture of 2-butanone and crocetin dialdehyde) was of good quality.[26]

For the bond length and angle analyses, it was necessary to set a minimum quality level for the crystallographic data. Accordingly, only structures with R1 values less than 0.09, and sp-carbon−sp-carbon bond lengths with standard deviations less than 0.01 Å, were considered. Compounds with disorder in the sp carbon chain were also rejected. On the basis of these criteria, no metrical parameters for C8-**5**, C8-**6**·$C_6H_{11}OH$, other inclusion adducts of

Chart 3. Crystallographically Characterized 1,3,5,7-Tetraynes with Platinum-Containing Endgroups (Part 1)

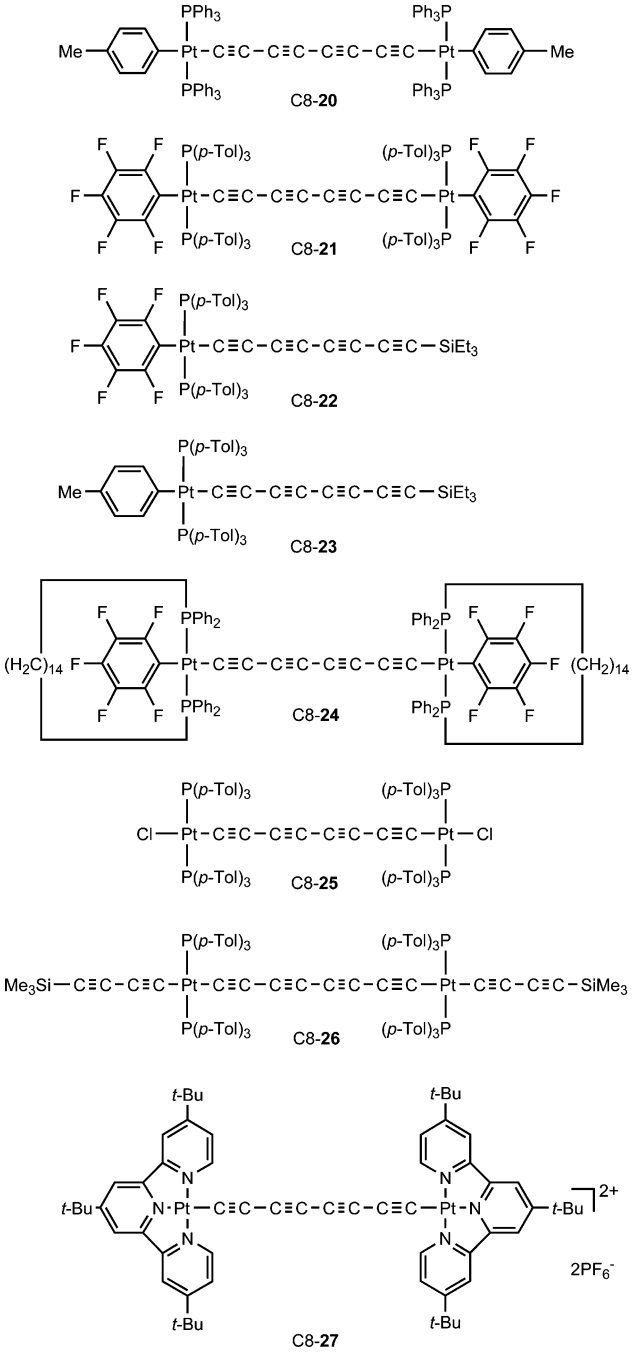

C8-**6**, C8-**13**, C8-**16**, C8-**17**, C8-**26**, C12-**6**, and C12-**9**·CH_2Cl_2 are analyzed. However, the conformations and packing motifs of some of these compounds are discussed. Thus, 28 good-quality structures of 1,3,5,7-tetraynes could be analyzed in their entirety, 18 with metal-containing endgroups and 10 with non-metal-containing endgroups.

3. Metrical and Unit Cell Parameters

Data for all compounds meeting the above criteria are presented in Tables 1−4. Most of the entries involving bond lengths and bond angles are self-explanatory and are analyzed below. For each compound, the space group, the volume of the unit cell, the number of molecules in the unit cell (*Z*), and the density are given. Where available, the refcode

Chart 4. Crystallographically Characterized 1,3,5,7-Tetraynes with Platinum-Containing Endgroups (Part 2)

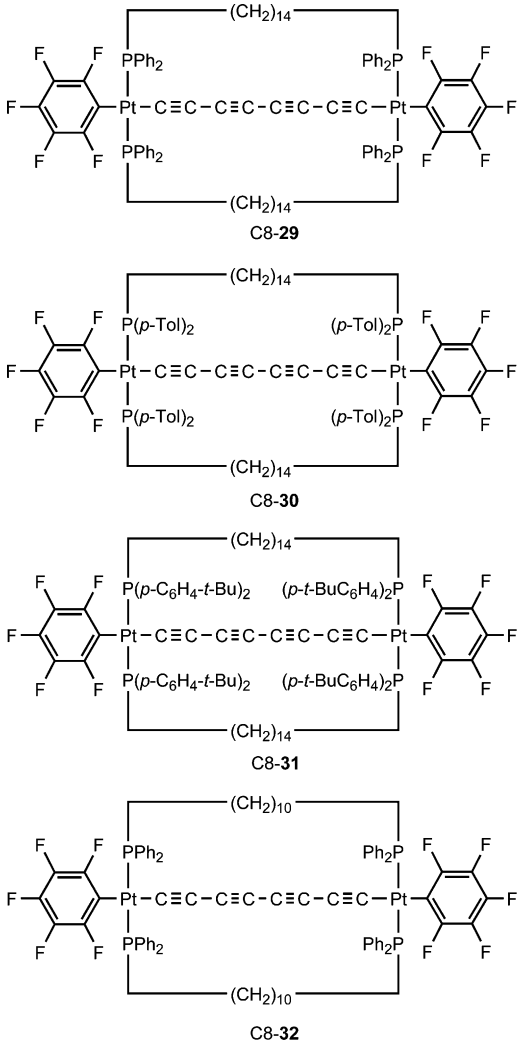

Chart 5. Crystallographically Characterized 1,3,5,7,9-Pentaynes, and 1,3,5,7,9,11-Hexaynes with Non-Metal-Containing Endgroups

A. Pentayne with non-Metal-Containing Endgroups

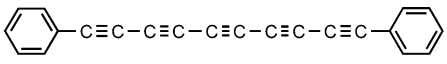

C10-**1**

B. Pentayne with Metal-Containing Endgroups

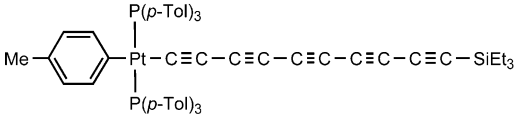

C10-**3**

C. Hexayne with non-Metal-Containing Endgroups

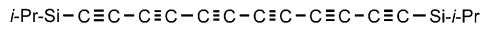

C12-**1**

Chart 6. Crystallographically Characterized 1,3,5,7,9,11-Hexaynes and 1,3,5,7,9,11,13,15-Octaynes with Metal-Containing Endgroups

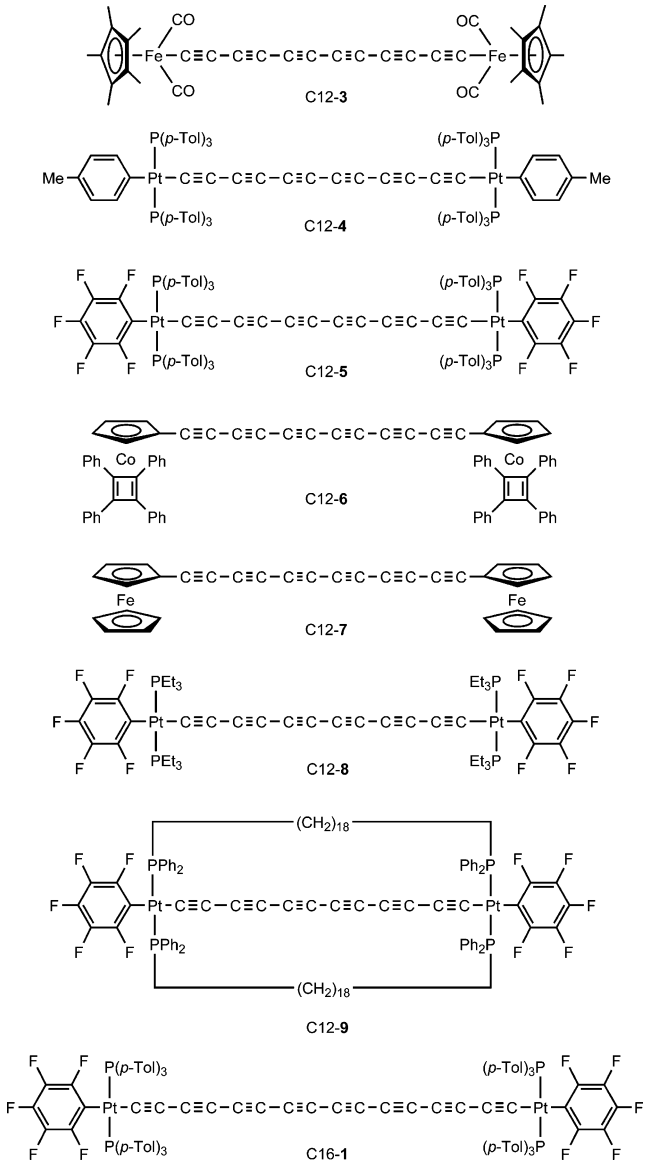

(REFC) for the Cambridge Structural Database is supplied. Analogous data for the poorer-quality structures are listed in Table S1 in the Supporting Information. Note that for noncentrosymmetric structures with identical endgroups, the designations X and X′ are arbitrary. The directionality could equally well be reversed, which would lead to minor changes in certain averages below.

4. Bond Length Analysis

The most important reference molecules for the compounds in Charts 1−6 and Tables 1−4 are ethyne and 1,3-butadiyne. Their C≡C bond lengths are 1.2033(2)[43] Å and 1.217(1)[44a]−1.20964 (14)[44b] Å, respectively. The sp-carbon/sp-carbon single bond length in 1,3-butadiyne is 1.384(2)[44a]−1.37081(16)[44b] Å. This is much shorter than the sp^3-carbon/sp^3-carbon single bond in ethane (1.54 Å),[45] reflecting the much greater s character in the constituent orbitals. An obvious initial question is how the bond lengths of the compounds in Charts 1−6 compare with these values.[46]

As summarized in Tables 1−3, the 1,3,5,7-tetraynes exhibit C≡C bond lengths that range from a low of 1.172(8) Å (for C8-**3**) to a high of 1.252(6) Å (for C8-**21**·C_7H_8), and C−C bond lengths that range from a low of 1.32 Å (for C8-**1**) to a high of 1.40(2) Å (for C8-**27**·4acetone). Thus, distances can vary by 0.08 Å, a considerable sum. Nonetheless, the esd values are usually too high to conclude, within a given compound, that one triple bond or one single bond is longer than another. An exception is C8-**21**·C_7H_8. Here the data are of excellent quality, and the C≡C linkage closer to the terminus is slightly longer (1.252(6) vs 1.209(6) Å). In contrast, there are other excellent-quality structures, such as C8-**22**, which show little or no hint of such a trend (1.224(5) vs 1.219(5) Å).

In an attempt to gain further insight, the average carbon−carbon bond lengths for all 1,3,5,7-tetraynes were calculated. The results are presented in Figure 1. In the left structure, the chain directionality from Tables 1−3 (e.g., the sequence C1−C8) is maintained, and the high and low values are given in smaller font sizes. As noted above, this sequence is arbitrary. Therefore, another set of averages are calculated about the midpoint of the chain, and these values are presented in the structures on the right side of Figure 1. In any event, the average lengths of the terminal and internal C≡C bonds are essentially identical (1.208 Å), and not substantially different from those of ethyne and 1,3-butadiyne. However, the innermost C−C bond is shorter than the other (1.360 vs 1.367 Å), and both are in turn shorter than the C−C bond of 1,3-butadiyne (1.384(2)−1.37081(16) Å).

As summarized in Table 4, the 1,3,5,7,9,11-hexaynes exhibit C≡C bond lengths that range from a low of 1.19(1) Å (for C12-**3**) to a high of 1.234(8) Å (for C12-**5**·4C_6H_6·EtOH), and C−C bond lengths that range from a low of 1.344(7) Å (for C12-**4**·2C_6H_6) to a high of 1.404(16) Å (for C12-**7**). Average bond lengths were similarly calculated, and are presented in Figure 1 together with data for the two 1,3,5,7,9-pentaynes and one 1,3,5,7,9,11,13,15-octayne. There are no obvious monotonic trends in the bond lengths for the hexaynes, although this might change as the number of compounds in the sample is expanded. There is also not yet enough data for many meaningful comparisons between tetraynes, pentaynes, hexaynes, octaynes, etc.

However, the average of all C≡C bond lengths in the octayne (1.216 Å) is greater than the corresponding averages for all hexaynes (1.212 Å), pentaynes (1.207 Å), and tetraynes (1.208 Å). The average of all C−C bond lengths in the octayne (1.351 Å) is shorter than the corresponding averages for all hexaynes (1.360 Å), pentaynes (1.364 Å), and tetraynes (1.365 Å). Thus, the C≡C bonds appear to become longer, and the C−C bonds shorter, as the chains lengthen. Since the incremental changes are progressively smaller, we suggest that the C≡C and C−C bond lengths approach *different* asymptotic values as the macromolecular limit of carbyne is approached. In other words, they do not converge to

Table 1. Summary of Crystallographic Data for the Tetraynes in Chart 1[a]

	C8-**1**[b,c]	C8-**2**	C8-**3**	C8-**4**	C8-**6**·BU·C[d,e]	C8-**7a**	C8-**7b**	C8-**8**	C8-**9**	C8-**10**
					Bond Lengths (Å)					
X−C1	1.41	1.819(7)	1.453(9)	1.417(2)	1.468(3)	1.433(3)	1.433(4)	1.429(6)	1.432(3)	2.033(4)
C1≡C2	1.19	1.20(1)	1.217(9)	1.189(2)	1.202(3)	1.200(3)	1.199(4)	1.203(7)	1.199(3)	1.208(6)
C2−C3	1.36	1.39(1)	1.377(9)	1.370(2)	1.368(3)	1.369(3)	1.368(5)	1.363(7)	1.372(3)	1.379(7)
C3≡C4	1.22	1.20(1)	1.172(8)	1.203(2)	1.210(3)	1.209(3)	1.209(4)	1.199(6)	1.207(3)	1.202(6)
C4−C5	1.32	1.33(1)	1.351(9)	1.373(2)	1.360(3)	1.365(3)	1.360(7)	1.378(10)	1.360(3)	1.361(7)
C5≡C6	1.22	1.20(1)	1.218(9)	1.203(2)	1.218(3)	1.203(3)	1.209(4)	1.199(6)	1.203(3)	1.194(6)
C6−C7	1.36	1.378(9)	1.362(10)	1.370(2)	1.359(3)	1.373(3)	1.368(5)	1.363(7)	1.370(3)	1.383(7)
C7≡C8	1.19	1.209(9)	1.202(8)	1.189(2)	1.206(3)	1.200(3)	1.199(4)	1.203(7)	1.197(3)	1.211(7)
C8−X′	1.41	1.822(7)	1.446(9)	1.417(2)	1.469(3)	1.432(3)	1.433(4)	1.429(6)	1.434(3)	2.030(5)
C1−C8, dist		8.88	8.87	8.89	8.91	8.91	8.91	8.90	8.88	8.93
C1−C8, sum	8.86	8.91	8.90	8.90	8.92	8.92	8.91	8.91	8.91	8.94
% contraction		0.34	0.34	0.11	0.11	0.11	0.00	0.11	0.34	0.11
X−X′, dist		12.49	11.76	11.72	11.82	11.77	11.77	11.76	11.74	12.99
X−X′, sum	11.68	12.55	11.80	11.73	11.86	11.78	11.78	11.77	11.77	13.00
% contraction		0.48	0.34	0.09	0.34	0.08	0.08	0.09	0.26	0.08
ξ (NLP)[f]		0.09531	0.07880	0.01939	0.07289	0.02202	0.01708	0.01842	0.07612	0.02091
					Bond Angles (deg)					
X−C1≡C2		178.1(6)	178.8(6)	178.4(2)	176.8(3)	179.1(2)	177.3(3)	178.5(5)	179.3(3)	176.5(4)
C1≡C2−C3		177.7(8)	177.6(6)	178.1(2)	177.1(3)	177.8(2)	178.4(3)	177.2(5)	178.5(3)	178.7(5)
C2−C3≡C4		177.4(7)	178.5(5)	177.7(2)	177.5(3)	177.5(2)	178.7(3)	177.3(5)	178.6(3)	178.8(5)
C3≡C4−C5		177.8(8)	177.4(6)	179.3(2)	178.5(3)	179.4(2)	178.6(4)	179.2(6)	177.1(3)	178.8(5)
C4−C5≡C6		176.9(8)	176.7(6)	179.3(2)	178.6(3)	179.5(3)	178.6(4)	179.2(6)	177.7(3)	178.6(6)
C5≡C6−C7		178.4(7)	178.9(6)	177.7(2)	179.4(3)	178.1(2)	178.7(3)	177.3(5)	177.4(3)	178.6(5)
C6−C7≡C8		178.6(7)	176.1(6)	178.1(2)	178.8(3)	177.1(2)	178.4(3)	177.2(5)	178.2(3)	178.3(5)
C7≡C8−X′		177.2(6)	179.4(6)	178.4(2)	178.7(3)	178.2(2)	177.3(3)	178.5(5)	179.1(3)	175.2(4)
avg angle		177.8	177.9	178.4	178.2	178.3	178.3	178.1	178.2	177.9
					Other Data					
space group	$P2_1/a$	$Pbcn$	$Pbcn$	$P2_1/n$	$P2_1/n$	$P2_1/c$	$P2_1/n$	$P\bar{1}$	$I2/a$	$P2/c$
V, Å^3	715	3423.7	2947(4)	642.0(2)	2540.1(4)	3699.7(4)	1896.1(3)	392.01(11)	4476.1(8)	1045.89(4)
Z	2	8	8	2	4	4	2	2	8	4
d_{calc}, g/cm^3	1.16	0.94	0.95	1.355	1.201[g]	1.018	0.993	1.729	1.076	2.422
R1		0.056	0.057	0.074	0.0819	0.0472	0.0679	0.053	0.0546	0.0283
REFC	DPOCTT	TMSIOC	YEXNIY	POVJEP	QAZHII	HOZSAQ02	HOZSAQ01	TIFXAH		WUWLAB
ref	14a	15	9	24	26	27	27	28	29	30

[a] All esd values are as reported, or rounded downward by one digit. [b] No bond angles or atomic coordinates were reported for C8-**1**. [c] Unit cell parameters have been reported for two polymorphs. Data for the second: $P2_1/a$; $V = 691$ Å^3; $Z = 2$; dcalc = 1.20 g/cm^3. In the Cambridge database, the space group is given as $P2_1/n$ (REFC = DPOCTT01). [d] C8-**6**·BU·C = C8-**6** cocrystallized with 2-butanone and 0.07 equiv of crocetin dialdehyde. [e] Parameters reported for C8-**6**·BU: $P2_1/n$; $V = 2525.2(35)$ Å^3; $Z = 4$; $d_{calc} = 1.154$ g/cm^3 for $C_{32}H_{38}O$; R1 = 0.1046. Structures of C8-**6**·BU and C8-**6**·BU·C are described as identical. [f] Nonlinearity parameter. [g] d_{calc} for $C_{32}H_{38}O·0.07(C_{20}H_{24}O_2)$.

a single common value. This is supported by additional evidence, as analyzed in other papers,[4−7] and implies a finite band-gap for carbyne. We propose that the longest C≡C and shortest C−C bonds in Tables 1−4, 1.252(6) Å (for C8-**21**·C_7H_8) and 1.33(1)-1.32 Å (for C8-**2** and C8-**1**), represent reasonable values for these limits.

A high-level computational study of the polyyne series H(C≡C)$_n$H ($n = 6-12$) shows analogous chain length effects.[12] For example, the HC≡C bonds lengthen from 1.2245 Å ($n = 6$) to 1.2247 Å ($n = 12$), while the HCC−C bonds contract from 1.3621 to 1.3613 Å. Similar trends are found elsewhere in the chains. Also, the C≡C bonds become longer as the midpoint of the chain is approached, and the C−C bonds shorter. The data for H(C≡C)$_{12}$H are presented in Figure 1. Here the C≡C bonds lengthen from 1.2247 to 1.2451 Å, while the C−C bonds contract from 1.3613 to 1.3389 Å. Unlike nearly all of the endgroups in Charts 1−6, hydrogen cannot participate in π interactions. Therefore, "endgroup effects" may perturb such monotonic trends near the chain termini.[47]

5. Classification of Carbon Chain Conformation

To help visualize some of the issues connected with bond angles, various limiting sp carbon chain conformations are first discussed. In contrast to the above treatment of bond lengths, the endgroups (and hence the X−C−C and C−C−X′ bond angles) are included in this analysis. As illustrated in Figure 2, one obvious limiting conformation is linear (**A**). However, none of the compounds in Tables 1−4 feature a perfectly linear polyyne. There are only a handful of bond angles greater than 179.5°, the largest being 179.9(7)° (for C8-**31**·5.5C_7H_8). When visualized from a proper perspective, angles of 178° are easily recognized as nonlinear. In any event, we suggest that the four compounds with average bond angles greater than or equal to 178.8° (C8-**12**, C8-**31**·5.5C_7H_8, C12-**1**, and C12-**7**) can be regarded as "essentially linear".

Another limiting conformation would be a symmetrically curved "bow", in which the sign of the slope changes (first derivative = 0) at the midpoint of the chain (**B**, Figure 2). A variant would be an "unsymmetric bow" (**C**), with a slope inversion elsewhere in

Table 2. Summary of Crystallographic Data for the Tetraynes in Charts 2 and 3[a]

	C8-**12**	C8-**14**	C8-**15**	C8-**18**	C8-**20**·4acetone·0.5$C_6H_4F_2$	C8-**21**·C_7H_8	C8-**22**	C8-**23**·CH_2Cl_2	C8-**24**·EtOH	C8-**25**·acetone	C8-**27**·4acetone
					Bond Lengths (Å)						
X−C1	1.425(9)	2.032(7)	2.016(8)	1.455(6)	2.011(4)	1.951(5)	1.986(3)	2.008(5)	1.985(5)	1.933(4)	1.935(13)
C1≡C2	1.19(1)	1.208(9)	1.214(11)	1.185(5)	1.218(6)	1.252(6)	1.224(5)	1.217(7)	1.221(8)	1.210(6)	1.210(16)
C2−C3	1.376(1)	1.35(1)	1.380(11)	1.383(6)	1.368(6)	1.365(6)	1.356(5)	1.344(8)	1.368(8)	1.368(6)	1.382(16)
C3≡C4	1.188(9)	1.21(1)	1.233(11)	1.211(5)	1.223(6)	1.209(6)	1.219(5)	1.221(8)	1.217(8)	1.199(6)	1.191(13)
C4−C5	1.37(1)	1.36(1)	1.338(11)	1.355(8)	1.367(9)	1.351(8)	1.355(5)	1.355(8)	1.370(12)	1.376(9)	1.40(2)
C5≡C6	1.188(9)	1.194(9)	1.242(12)	1.211(5)	1.223(6)	1.209(6)	1.211(5)	1.203(8)	1.217(8)	1.199(6)	1.191(13)
C6−C7	1.376(1)	1.37(1)	1.337(12)	1.383(6)	1.368(6)	1.365(6)	1.367(5)	1.358(8)	1.368(8)	1.368(6)	1.382(16)
C7≡C8	1.19(1)	1.20(1)	1.223(11)	1.185(5)	1.218(6)	1.252(6)	1.202(5)	1.225(8)	1.221(8)	1.210(6)	1.210(16)
C8−X′	1.425(9)	1.848(9)	1.439(12)	1.455(6)	2.011(4)	1.951(5)	1.848(4)	1.833(6)	1.985(5)	1.933(4)	1.935(13)
C1−C8, dist	8.88	8.872(9)	8.89(2)	8.90	8.98	9.00	8.86	8.92	8.98	8.93	8.97
C1−C8, sum	8.88	8.89	8.97	8.91	8.99	9.00	8.93	8.92	8.98	8.93	8.97
% contraction	0.00	0.20	0.90	0.11	0.11	0.00	0.79	0.00	0.00	0.00	0.00
X−X′, dist	11.73	12.74	12.22	11.80	13.00	12.90	12.62	12.73	12.94	12.78	12.84
X−X′, sum	11.73	12.77	12.42	11.82	13.01	12.91	12.77	12.76	12.95	12.80	12.84
% contraction	0.00	0.24	1.64	0.17	0.08	0.08	1.19	0.24	0.08	0.16	0.00
ξ (NLP)[b]	0.00901	0.05519	0.16750	0.02835	0.01564	0.01785	0.15396	0.04936	0.02386	0.04174	0.01234
					Bond Angles (deg)						
X−C1≡C2	179.5(5)	176.4(6)	174.5(7)	178.9(5)	178.0(4)	177.6(4)	179.3(3)	175.8(5)	175.9(6)	178.6(4)	178.5(13)
C1≡C2−C3	177.9(6)	177.4(8)	170.0(9)	176.7(5)	176.5(5)	179.2(5)	177.3(4)	178.4(6)	178.3(8)	174.6(5)	179.5(16)
C2−C3≡C4	179.6(6)	178.2(8)	176.9(9)	177.1(5)	177.8(5)	177.1(5)	178.4(4)	178.5(7)	177.8(8)	174.9(6)	177.2(12)
C3≡C4−C5	179.6(6)	176.4(8)	173.6(10)	177.5(6)	179.5(9)	178.5(6)	175.1(4)	177.8(7)	179.0(11)	178.3(7)	179.0(19)
C4−C5≡C6	179.6(6)	178.9(8)	178.1(10)	177.5(6)	179.5(9)	178.5(6)	175.7(4)	179.0(8)	179.0(11)	178.3(7)	179.0(19)
C5≡C6−C7	179.6(6)	175.9(8)	177.6(10)	177.1(5)	177.8(5)	177.1(5)	174.5(4)	177.1(7)	177.8(8)	174.9(6)	177.2(12)
C6−C7≡C8	177.9(6)	179(1)	178.8(10)	176.7(5)	176.5(5)	179.2(5)	177.7(4)	177.2(7)	178.3(8)	174.6(5)	179.5(16)
C7≡C8−X′	179.5(5)	178.0(9)	175.8(10)	178.9(5)	178.0(4)	177.6(4)	178.6(4)	173.3(5)	175.9(6)	178.6(4)	178.5(13)
avg angle	179.2	177.5	175.7	177.6	178.0	178.1	177.1	177.1	177.8	176.6	178.6
					Other Data						
space group	*C*2/*m*	$P2_1/n$	$P2_1/n$	$P2_1/c$	$P\bar{1}$	$P2_1/c$	$P\bar{1}$	$P2_1/n$	$P\bar{1}$	$P2_1/c$	$P2_1/c$
V, Å^3	1029.0(5)	3743(2)	3480(3)	1525.6(4)	2246.2(2)	4948(2)	2828.5(1)	5848.96(19)	2318.7(8)	4429.41(7)	4074.3(14)
Z	4	4	4	2	1	2	2	4	1	2	2
d_{calc}, g/cm^3	1.504	1.389	1.529(1)	1.355	1.484	1.430	1.388	1.353	1.432	1.418	1.477
R1	0.029	0.0329	0.0314	0.0562	0.0396	0.0374	0.0268	0.0413	0.0426	0.0317	0.0403
REFC	RARNUT	NOHVUB	BEJCEY		XAWBEC	IBITUI	HUXYII				WABZAB
ref	17	13	31	29	33	34	35	36	36	36	37

[a] All esd values are as reported, or rounded downward by one digit. [b] Nonlinearity parameter.

Table 3. Summary of Crystallographic Data for the Tetraynes in Chart 4[a]

	C8-**29**·1.5C_6H_6	C8-**29**·1.5C_7H_8	C8-**30**	C8-**31**·2C_7H_8	C8-**31**·5.5C_7H_8	C8-**32**·4C_7H_8	C8-**32**·2$CHCl_3$
			Bond Lengths (Å)				
X−C1	1.994(3)	1.987(4)	1.991(8)	1.989(7)	1.988(4)	2.014(6)	1.998(5)
C1≡C2	1.209(5)	1.215(7)	1.211(9)	1.220(9)	1.205(6)	1.192(8)	1.219(6)
C2−C3	1.368(5)	1.365(7)	1.345(10)	1.356(10)	1.369(6)	1.366(8)	1.359(7)
C3≡C4	1.216(5)	1.214(7)	1.201(9)	1.202(10)	1.206(6)	1.208(8)	1.224(7)
C4−C5	1.354(5)	1.360(7)	1.363(10)	1.377(15)	1.360(6)	1.361(9)	1.362(6)
C5≡C6	1.207(5)	1.207(7)	1.198(9)	1.202(10)	1.209(6)	1.215(8)	1.212(6)
C6−C7	1.368(5)	1.360(7)	1.372(10)	1.356(10)	1.356(6)	1.368(8)	1.369(6)
C7≡C8	1.207(5)	1.212(6)	1.222(9)	1.220(9)	1.220(6)	1.210(8)	1.209(6)
C8−X′	2.003(3)	1.994(4)	1.987(7)	1.989(7)	1.983(4)	1.999(6)	2.002(4)
C1−C8, dist	8.88	8.89	8.85	8.92	8.92	8.92	8.87
C1−C8, sum	8.93	8.93	8.91	8.93	8.93	8.92	8.95
% contraction	0.56	0.45	0.68	0.11	0.11	0.00	0.90
X−X′, dist	12.75	12.77	12.70	12.88	12.89	12.91	12.64
X−X′, sum	12.93	12.91	12.89	12.91	12.90	12.93	12.95
% contraction	1.41	1.11	1.50	0.23	0.08	0.15	2.45
ξ (NLP)[b]	0.15694	0.13900	0.17226	0.03096	0.03634	0.02825	0.21115
			Bond Angles (deg)				
X−C1≡C2	171.7(3)	175.9(5)	178.8(6)	175.7(7)	179.3(4)	174.0(6)	171.1(4)
C1≡C2−C3	174.1(4)	178.9(6)	176.4(8)	175.6(8)	178.3(5)	178.2(8)	176.4(6)
C2−C3≡C4	176.3(4)	178.4(6)	176.0(8)	179.4(10)	179.9(7)	178.3(7)	177.4(5)
C3≡C4−C5	178.5(5)	178.2(6)	175.3(8)	178.8(12)	178.5(6)	178.5(9)	177.4(5)
C4−C5≡C6	176.9(5)	177.0(6)	176.0(8)	178.8(12)	179.9(6)	179.6(9)	177.0(5)
C5≡C6−C7	177.3(4)	177.3(6)	177.9(8)	179.4(10)	178.5(5)	178.5(8)	175.0(5)
C6−C7≡C8	177.5(4)	172.8(5)	178.2(8)	175.6(8)	179.1(5)	177.5(7)	173.5(5)
C7≡C8−X′	178.0(3)	171.6(4)	171.5(6)	175.7(7)	179.3(4)	176.7(6)	169.4(4)
avg angle	176.3	176.2	176.3	177.4	179.1	177.7	174.7
			Other Data				
space group	$P\bar{1}$	$P\bar{1}$	$P\bar{1}$	$P2_1/c$	$P\bar{1}$	$P2_1/n$	$P\bar{1}$
V, Å^3	4668.33(13)	4604.8(16)	4713.52(16)	6445(2)	7690.11(13)	9995.45(15)	4275.6(15)
Z	2	2	2	2	2	4	2
d_{calc}, g/cm^3	1.473	1.506	1.456	1.333	1.256	1.468	1.616
R1	0.0320	0.0342	0.0415	0.0498	0.0437	0.0488	0.0355
REFC		MOHGUL	MOHHAS		MOHHOG	MOHHIA	MOHHEW
ref	38	38	38	38	38	38	38

[a] All esd values are as reported, or rounded downward by one digit. [b] Nonlinearity parameter.

the chain. Intuitively, the former might be expected to be more common when the endgroups are identical, and the latter when they are not. Rigorously, a symmetric bow should exhibit a symmetry element such as a C_2 axis or mirror plane. However, for polyynes with a slope change near the midpoint of the two innermost carbon atoms and similar metrical parameters on each side, we do not impose this requirement.

Other possible conformations feature inflection points (second derivative = 0). Here we define two variants. In one (**D**), the X−C1−C2 and C1−C2−C3 angles are close to 180°, such that the inflection point appears as a kink in an otherwise fairly linear chain. In the other (**E**), the X−C1−C2 and/or C1−C2−C3 linkages are less than 178°, such that an S-shape is evident. As analyzed below, the latter is somewhat more common. With **B**-**E**, secondary conformational features such as spirals or coiling are also conceivable, and hints of such motifs will be evident in some structures below.

In principle, a randomly bent chain should be possible, as represented by **F**. Interestingly, nature appears to avoid this less aesthetic conformation, which has been found in only one high-quality structure to date (below). Nonetheless, it has been suggested that carbyne might bend or coil and thermally isomerize to fullerenes or other carbon allotropes.[9,10] Indeed, the bending force constants for X−C≡C and C≡C−C linkages are relatively weak. DFT calculation on model polyynes show that only a few kcal/mol are needed to produce distortions that match the most bent compounds described below.[47]

6. Bond Angle and Chain Linearity Analysis

We are unaware of any previous attempts to quantify the degree of linearity in molecules or objects that can adopt the types of conformations in Figure 2. Importantly, the bond angles in Tables 1−4 do not provide a direct measure or a reliable qualitative indicator. For example, even when every bond angle is only slightly less than 180°, if the bending always has the same directional sense, a distinctly curved system results. If the directional sense of the bending changes from bond to bond, giving a zigzag pattern, a much more linear system results.

Interestingly, there is a somewhat greater tendency for bending near the ends of the chains. The averages of all X−C1−C2 and $C_{\omega-1}-C_{\omega}-X'$ bond angles (174.4°) are lower than the averages of all C1−C2−C3 and $C_{\omega-2}-C_{\omega-1}-C_{\omega}$ bond angles (177.2°), which are in

Table 4. Summary of Crystallographic Data for the Pentaynes, Hexaynes, and Octaynes in Charts 5 and 6[a]

	C10-**1**	C10-**3**	C12-**1**	C12-**3**	C12-**4**·2C_6H_6	C12-**5**·4C_6H_6·EtOH	C12-**7**	C12-**8**	C16-**1**·10C_6H_6
					Bond Lengths (Å)				
X−C1	1.423(7)	1.992(6)	1.8522(16)	1.878(9)	1.990(3)	1.972(6)	1.418(10)	1.999(4)	1.981(2)
C1≡C2	1.192(7)	1.219(7)	1.206(2)	1.23(1)	1.233(4)	1.234(8)	1.224(10)	1.205(6)	1.220(3)
C2−C3	1.369(7)	1.375(8)	1.368(2)	1.36(1)	1.358(4)	1.361(8)	1.349(11)	1.361(5)	1.355(3)
C3≡C4	1.206(7)	1.200(8)	1.208(2)	1.20(1)	1.210(5)	1.209(8)	1.204(10)	1.224(5)	1.214(3)
C4−C5	1.368(7)	1.344(8)	1.356(2)	1.35(1)	1.356(5)	1.363(8)	1.347(11)	1.363(5)	1.350(3)
C5≡C6	1.21(1)	1.220(8)	1.2090(19)	1.22(1)	1.211(5)	1.216(7)	1.196(9)	1.204(5)	1.217(4)
C6−C7	1.368(7)	1.355(9)	1.358(3)	1.35(1)	1.344(7)	1.358(8)	1.404(16)	1.358(7)	1.349(3)
C7≡C8	1.206(7)	1.209(8)	1.2090(19)	1.23(1)	1.211(5)	1.210(7)	1.196(9)	1.204(5)	1.212(3)
C8−C9	1.369(7)	1.363(9)	1.356(2)	1.36(1)	1.356(5)	1.356(7)	1.347(11)	1.363(5)	1.349(5)
C9≡C10	1.192(7)	1.213(9)	1.208(2)	1.19(1)	1.210(5)	1.208(7)	1.204(10)	1.224(5)	1.212(3)
C10−X′	1.423(7)	1.842(7)							
C10−C11			1.368(2)	1.38(1)	1.358(4)	1.374(7)	1.349(11)	1.361(5)	1.349(3)
C11≡C12			1.206(2)	1.20(1)	1.233(4)	1.223(7)	1.224(10)	1.205(6)	1.217(4)
C12−X′			1.8522(16)	1.888(1)	1.990(3)	1.983(5)	1.418(10)	1.999(4)	
C12−C13									1.350(3)
C13≡C14									1.214(3)
C14−C15									1.355(3)
C15≡C16									1.220(3)
C16−X′									1.981(2)
C1−C_ω, dist	11.48	11.47	14.05	13.94	14.05	13.66	14.04	14.04	19.15
C1−C_ω, sum	11.48	11.50	14.05	14.07	14.08	14.11	14.04	14.07	19.18
% contraction	0.00	0.25	0.00	0.93	0.21	3.29	0.00	0.21	0.16
X−X′, dist	14.32	15.26	17.75	17.56	17.96	17.009(6)	16.88	18.0307(3)	23.071(4)
X−X′, sum	14.33	15.33	17.76	17.84	18.06	18.07	16.88	18.07	23.15
% contraction	0.07	0.43	0.06	1.59	0.56	6.24	0.00	0.22	0.34
ξ (NLP)[b]	0.04750	0.08129	0.01629	0.12778	0.06208	0.41467	0.01002	0.03378	0.05062
					Bond Angles (deg)				
X−C1≡C2	178.1(6)	176.4(5)	177.88(15)	175.2(6)	174.0(3)	172.9(5)	178.3(7)	175.5(6)	175.7(2)
C1≡C2−C3	178.5(7)	174.1(6)	179.3(2)	172.7(8)	174.5(4)	173.2(7)	178.5(7)	179.3(18)	176.9(3)
C2−C3≡C4	178.3(6)	177.8(6)	178.91(19)	175.5(8)	178.6(4)	178.3(7)	179.3(7)	174(2)	178.2(3)
C3≡C4−C5	178.7(7)	177.4(7)	178.50(18)	176.8(9)	178.3(4)	175.6(7)	179.7(7)	173(2)	178.0(3)
C4−C5≡C6	178.5(9)	178.7(7)	178.80(18)	176.3(9)	177.5(4)	175.3(6)	178.8(7)	176(2)	178.7(3)
C5≡C6−C7	178.5(9)	177.2(7)	179.3(2)	177(1)	178.9(6)	175.7(6)	179.5(8)	178.4(10)	179.1(3)
C6−C7≡C8	178.7(7)	177.4(7)	179.3(2)	178(1)	178.9(6)	175.7(6)	179.5(8)	178.4(10)	178.3(3)
C7≡C8−C9	178.3(6)	179.3(8)	178.80(18)	176.9(9)	177.5(4)	175.3(6)	178.8(7)	176(2)	179.3(3)
C8−C9≡C10	178.5(7)	177.7(8)	178.50(18)	175.1(9)	178.3(4)	173.4(6)	179.7(7)	173(2)	179.3(3)
C9≡C10−X	178.1(6)	175.3(7)							
C9≡C10−C11			178.91(19)	173.8(9)	178.6(4)	176.2(6)	179.3(7)	174(2)	178.3(3)
C10−C11≡C12			179.3(2)	171.7(9)	174.5(4)	171.8(6)	178.5(7)	179.3(18)	179.1(3)
C11≡C12−X′			177.88(15)	173.3(7)	174.0(3)	171.6(5)	178.3(7)	175.5(6)	
C11≡C12−C13									178.7(3)
C12−C13≡C14									178.0(3)
C13≡C14−C15									178.2(3)
C14−C15≡C16									176.9(3)
C15≡C16−X′									175.7(2)
avg angle	178.4	177.1	178.8	175.2	177.0	174.6	179.0	176.0	178.0
					Other Data				
space group	$P2_1/n$	$P\bar{1}$	$P2_1/c$	$P2_1/c$	$P\bar{1}$	$P21/c$	$C2/m$	$C2$	$P\bar{1}$
V, Å^3	784	2766.2(2)	1537.4(2)	3124(2)	2544.70(9)	11542.4(2)	1145.7(3)	2673.2(1)	3686.5(1)
Z	2	2	2	4	1	4	2	2	1
d_{calc}, g/cm^3	1.161	1.357	0.991	1.357	1.364	1.659	1.49	1.666	1.313
R1	0.087	0.0399	0.0402	0.0857	0.0375	0.0388	0.044	0.0237	0.0273
REFC	DPDECP01			LAQBOU	XAWBAY	IBIVEU	HUNFOL		IBIVAQ
ref	18	36	29	39	33	34	41	34	34

[a] All esd values are as reported, or rounded downward by one digit. [b] Nonlinearity parameter.

turn lower than the average of the remaining C−C−C bond angles (177.8°). The lowest values in each category are 171.1(4)° (X−C1−C2, C8-**32**·2$CHCl_3$), 169.4(4)° ($C_{\omega-1}$−C_ω−X′, C8-**32**·2$CHCl_3$), 170.0(9)° (C1−C2−C3, C8-**15**), and 171.7(9)° ($C_{\omega-2}$−$C_{\omega-1}$−C_ω, C12-**3**). However, in calcium, strontium, and barium alkynyl complexes, in which the metal bonding orbitals have very high s character, much lower X−C1−C2 bond angles can be found (Ca, 162.4(5)−164.0(5)°; Sr, 158.9(3)−159.7(3)°; Ba, 126.6(3)−141.3(3)°).[48]

One qualitative measure of nonlinearity can be derived from the bond lengths. First, distances between the endgroups X/X′ are calculated from the atomic coordinates. These values are summarized in Tables 1−4. These are in turn compared to the sums of the lengths of the bonds connecting the endgroups.

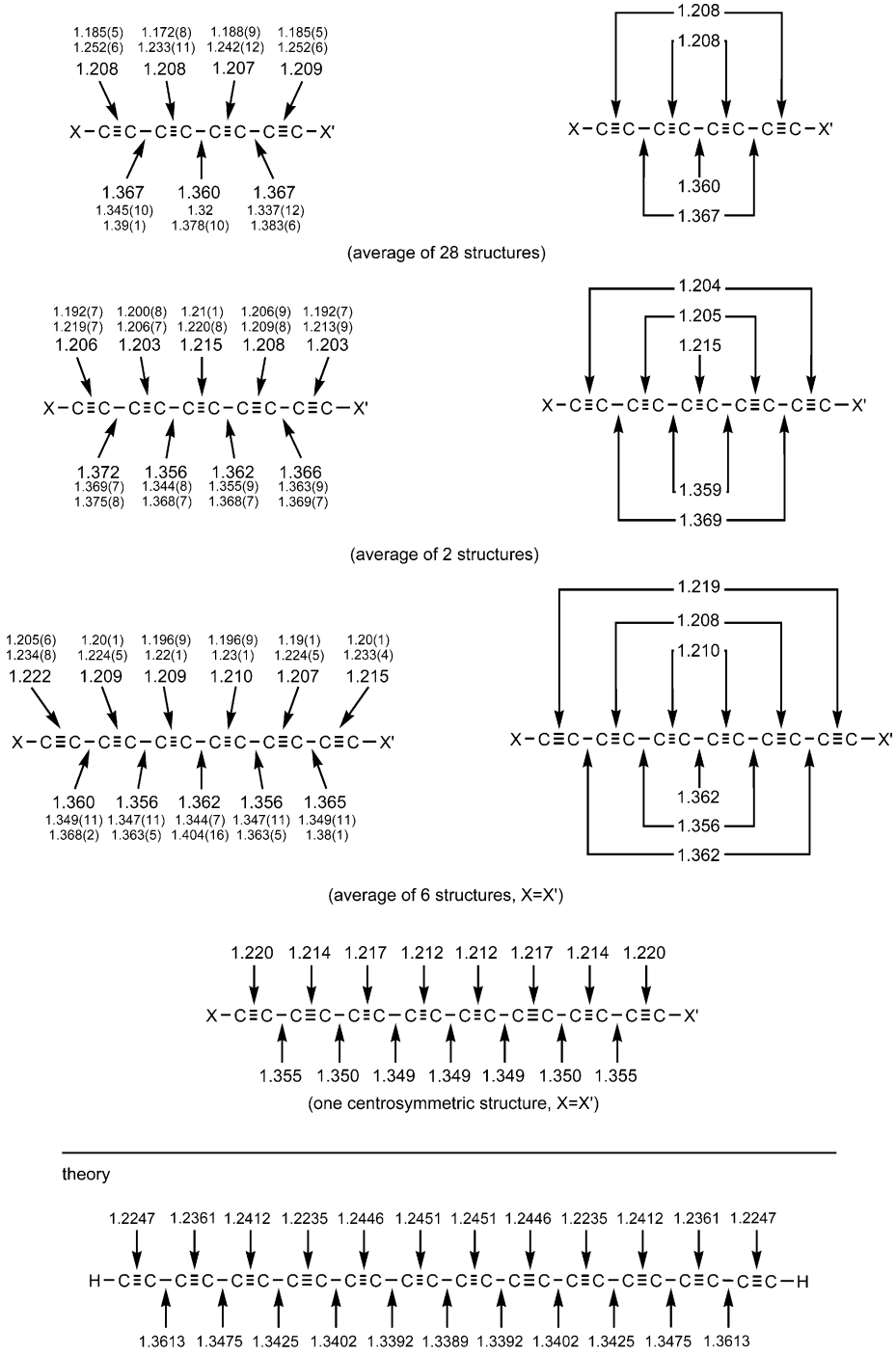

Figure 1. Average carbon−carbon bond lengths in polyynes (Å; high and low values are given in smaller font sizes).

In the limit of a linear chain (**A**), the values are equal. In all other cases, the X/X′ distances are shorter. A "percent contraction" can then be calculated. Since the endgroups in Charts 1−6 are so heterogeneous, with X−C1 and C_ω−X′ bond lengths that depend on the identity of X, it may in some cases be advantageous to compare the distances between the terminal sp carbons C1/C_ω and the sum of the intervening bond lengths. These values are also provided.

The 1,3,5,7-tetraynes in Chart 1, which feature non-metal-containing endgroups, all show a very high degree of linearity, as evidenced by the close correspondence of the X−X′ or C1−C8 distances and the sums of the X−X′ or C1−C8 bond lengths (<0.48% and <0.34% contractions, respectively). The longer polyynes, C10-**1**, C12-**1**, C12-**7**, in which the sp carbon chains terminate with carbon−carbon or carbon−silicon bonds, are similar (X/X′ and C1/C_ω contractions of 0.07/0.00%, 0.06/0.00%, and 0.00/0.00%). Many of the tetraynes in Charts 2−4 also have high degrees of linearity, but C8-**15**, C8-**22**, C8-**29**·1.5C_6H_6, C8-**29**·1.5C_7H_8, C8-**30**, and C8-**32**·2$CHCl_3$ do not (X/X′ and C1/C_ω contractions of 1.64/0.90, 1.19/0.79, 1.41/0.56, 1.11/0.45, 1.50/0.68, and 2.45/0.90%).

By this criterion, C8-**32**·2$CHCl_3$ is the least linear 1,3,5,7-octatetrayne, and C12-**5**·4C_6H_6·EtOH is the least linear 1,3,5,7,9,11-hexayne (X/X′ and C1/C_ω contractions 6.24/3.29%). The structure of the latter, which features the symmetric bow conformation **B**, is depicted below. However, this algorithm clearly

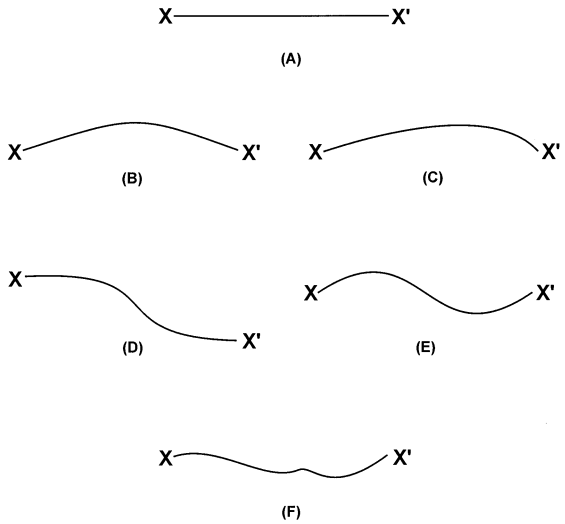

Figure 2. Types of carbon chain conformations: (A) linear, (B) symmetric bow, (C) unsymmetric bow, (D) kinked, (E) S-shaped, (F) random.

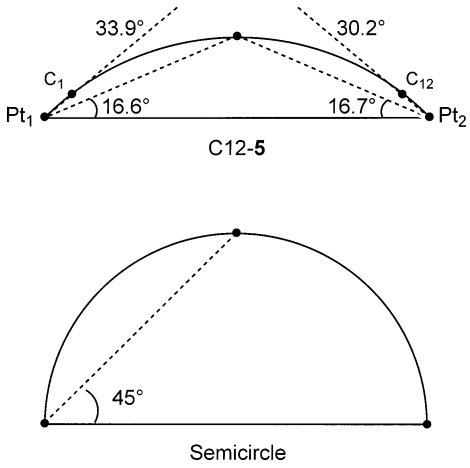

Figure 3. Curvature analysis for the symmetric bow conformation.

confers greater weight to bow-type distortions such as in **B** and **C**. Given equal bond lengths and angles, the X/X′ groups will always be further apart and closer to the sum of the bond lengths in the kinked and S-shaped conformations **D** and **E**.

For compounds with the symmetric bow conformation **B**, curvature can be quantified with reference to a semicircle. A vector is first defined between the endgroups, and the midpoint of the sp carbon chain is then calculated. As shown in Figure 3, a second vector is defined between an endgroup and the midpoint. The angle between the two vectors is then calculated. In the case of a semicircle, the value is 45°. For the most bow-shaped molecule in Charts 1−6, noncentrosymmetric C12-**5**·$4C_6H_6$·EtOH, the value is 16.6−16.7°.[5,34,49] Thus, the $PtC_{12}Pt$ chain can be regarded as having "37% of the curvature of a semicircle".

Is it possible to define a meaningful measure of nonlinearity that is independent of chain conformation? We propose a "nonlinearity-parameter" (NLP), ξ, which is named in accord with the least linear character in the Greek alphabet (lower case xi) and calculated as follows. First, the least-squares line for the $X(C{\equiv}C)_nX'$ assembly is determined. Note that the line is not constrained to pass through X/X′. In this determination, the square of the deviation of every atom from the line is automatically obtained. These squares are summed and divided by the square of the X/X′ distance to normalize (at least in part) for the chain length. This affords a dimensionless number. Finally, the square root is taken (since squares of distances were employed), giving the parameter ξ.[50] The larger the number, the greater the deviation from linearity. The results are summarized in Tables 1−4.

The 1,3,5,7-tetraynes in Chart 1, which by the criteria used above show high degrees of linearity, give ξ values ranging from 0.01708 (for C8-**7b**) to 0.09531 (for C8-**2**), or a factor greater than five (Table 1). There is no correlation with the average bond angle, or the percent contractions in X/X′ distances. The six tetraynes that were described above as much less linear, all of which are from Charts 2−4 (C8-**15**, C8-**22**, C8-**29**·$1.5C_6H_6$, C8-**29**·$1.5C_7H_8$, C8-**30**, C8-**32**·$2CHCl_3$), give much higher values (0.16750, 0.15396, 0.15694, 0.13900, 0.17226, 0.21115, respectively). The tetrayne with the highest ξ, C8-**32**·$2CHCl_3$, is also the most distorted by the other criteria analyzed above. The remaining tetraynes in Charts 2−4 give ξ values less than 0.05519, and the most linear is C8-**12** (0.00901).

Turning to the higher polyynes, the largest ξ values are found with hexaynes C12-**3** (0.12778) and C12-**5**·$4C_6H_6$·EtOH (0.41467). The latter compound exhibits by far the highest ξ value of all (nearly twice that of C8-**32**·$2CHCl_3$), as well as the largest percentage contraction in X/X′ distance (more than twice that of C8-**32**·$2CHCl_3$). The two hexaynes noted above as essentially linear, C12-**1** (average bond angle 178.8°) and C12-**7** (average bond angle 179.0°), give ξ values of 0.01629 and 0.01002.

To further test and calibrate this parameter, the idealized "conformation tree" shown in Figure 4 was constructed with bond lengths of 1.3 Å and angles of 178.0°. In principle, all possible chain conformations can be depicted from a common origin or root, ranging from a zigzag branch approximating a linear chain to a maximally curved branch that corresponds to a symmetric bow. Figure 4 depicts both of these extremes, and an intermediate S-shaped conformation. Branches of 10, 14, and 18 atoms were analyzed, corresponding to tetraynes, hexaynes, and octaynes, respectively.

The ξ values computed for the zigzag (approximately linear), S-shaped, and symmetric bow conformations of tetraynes (black chains) are 0.00307, 0.02151, and 0.04466, respectively (% contractions 0.02, 0.08, 0.41). The ξ value of the symmetric bow is about twice that of the S-shaped conformer, which is in turn about seven times that of the zigzag conformer. The corresponding values for the model hexaynes (black and red chains) are 0.00251, 0.03737, and 0.07277, respectively (% contractions 0.01, 0.19, 0.86). Those for the symmetric bow and S-shaped conformer increase, but maintain a ca. 2:1 relationship. That of the zigzag conformation decreases slightly. The ξ values for the for the model octaynes

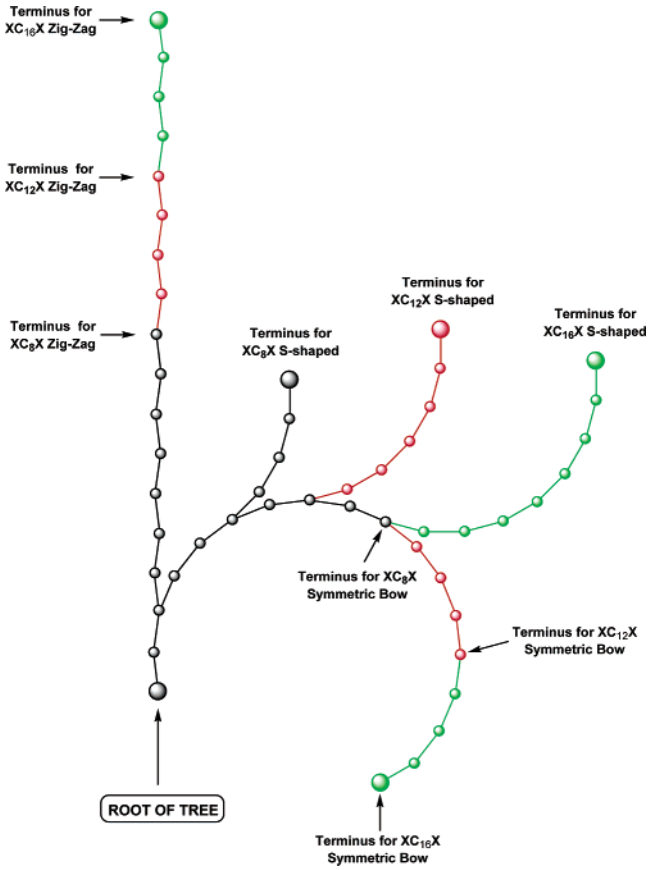

Figure 4. Conformational "tree" for calibration of the nonlinearity parameter (NLP) ξ (calculated for bond lengths of 1.30 Å and bond angles of 178°; the latter are made more concave in the figure for clarity).

(chains terminating in green), 0.00218, 0.05592, and 0.1052 (% contractions 0.00, 0.34, 1.48), continue these trends.

Hence, a chain of atoms with a symmetric bow conformation always gives a higher ξ value than one with a S-shaped conformation that is comprised of identical bond lengths and angles (ca. 2:1 ratio for the cases in Figure 4). When such chains are extended, the degree of nonlinearity and the ξ values increase. In the case of zigzag conformations, the much smaller ξ values are not so dependent upon chain length. As the number of atoms increases, the individual deviations from nonlinearity becomes less with respect to the length, and ξ values decrease slightly. Despite certain nonidealities, we believe that the parameter ξ represents the best means of comparing nonlinearity. It is relatively easy to compute, rather intuitive, and much less esoteric than several alternatives.[51]

7. Chain Conformations: Specific Examples

In this section, phenomena described in the previous two sections are illustrated with specific structures. First, two views of one of the molecules described as "essentially linear" or closely approximating conformation **A** (Figure 2), the diferrocenyl tetrayne C8-**12**, are given in Figure 5. This centrosymmetric compound has the lowest ξ value (0.00901), and the smallest bond angle is 177.9(6)°

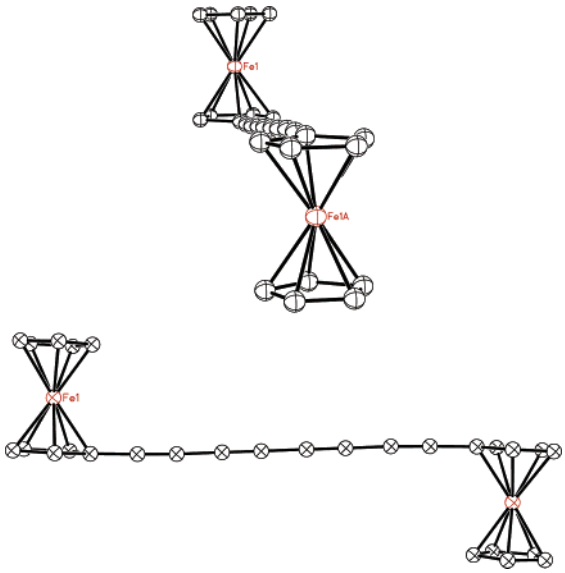

Figure 5. Carbon chain conformation in C8-**12** (**A**, "essentially linear").

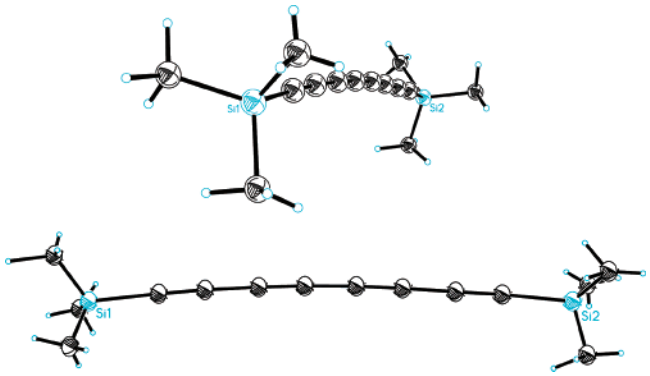

Figure 6. Carbon chain conformation in C8-**2** (**B**, symmetric bow).

(C1−C2−C3 and C6−C7−C8). This bending is in our eyes barely perceptible when the molecule is viewed from the optimal perspective (Figure 5, bottom). The diferrocenyl *hexa*yne C12-**7** exhibits a similar degree of linearity (ξ 0.01002).

Turning to non-metal-containing systems (Charts 1 and 5A,C), the tetraynes C8-**2** and C8-**3**, which feature approximately isostructural trimethylsilyl and *tert*-butyl endgroups, exhibit gently curved, symmetric bow-shaped conformations **B** (ξ 0.09531, 0.07880). The former is illustrated in Figure 6. In neither case does a C2 axis or mirror plane pass through the midpoint of the chain. However, the deviations from ideality are small. As summarized in Table 1, the space groups are identical, and the average bond angles and C1/C8 contractions nearly so. The unit cell dimensions are also quite close, with the volume of C8-**2** approximately 12% greater. This, and the greater X/X′ contraction in C8-**2**, are consistent with the longer silicon−carbon bonds. Since the longer bonds extend the silicon atoms further from the least squares line, the ξ value is also greater.

Symmetric bow conformations (**B**) are also found for tetraynes C8-**6**·BU·C and C8-**9** (ξ 0.07289, 0.07612). In the latter, the planes of the *p*-(*tert*-butyl)-phenyl endgroups are twisted by 67°, and define angles of 85.3° and 18.5° with the plane of the bow.

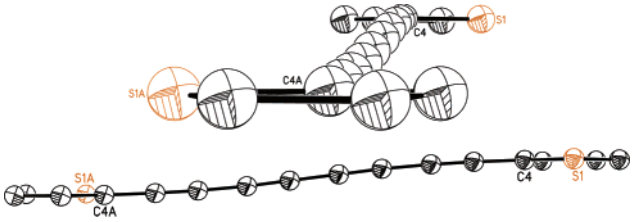

Figure 7. Carbon chain conformation in C8-**4** (**D**, kinked).

This contrasts with the parallel phenyl endgroups in the pentayne C10-**1** (ξ 0.04750). This centrosymmetric molecule exhibits a gentle version of the S-shaped conformation **E**. The plane of the S defines a 17.9° angle with that of each phenyl ring. The atomic coordinates of the lower homolog, tetrayne C8-**1**,[14] have never been published, precluding comparison or analysis. Although the centrosymmetric hexayne C12-**1** was described in the previous section as "essentially linear" (ξ 0.01629), upon close inspection a very slight S shape can be discerned.

According to the above analysis, the thienyl-substituted tetrayne C8-**4** exhibits a kinked conformation **D**. Views of this centrosymmetric structure are given in Figure 7. The smallest bond angle (177.7(2)°) is found for C2−C3−C4 and C5−C6−C7. The planes of the thienyl rings are parallel, but displaced by ca. 0.98 Å since the kink does not lie in the plane of the rings. The ξ value (0.01939) is lower and the average bond angle (178.4°) higher than with the bow-shaped tetraynes C8-**2** and C8-**3**. Both polymorphs of C8-**7** (**a**,**b**), as well as C8-**8**, adopt similar kinked conformations (ξ 0.02202, 0.01708, 0.01842). The conformation of the ditellurium compound C8-**10**, the crystal lattice of which is analyzed further below, is best described as random (**F**, Figure 2; ξ 0.02091).

Turning to metal-containing endgroups of all sp carbon chain lengths (Charts 2−4, 5B, 6), we first illustrate the compound with the highest degree of nonlinearity, hexayne C12-**5**·4C_6H_6·EtOH (ξ 0.41467). As shown in Figure 8, it adopts the symmetric bow conformation **B**. Note that end-on perspectives (Figure 8, top) visually enhance any curvature or distortions. In contrast, the centrosymmetric hexayne C12-**8**, which has aliphatic phosphine ligands, exhibits a kinked conformation **D** as shown in Figure 9. Here, the C2−C3−C4, C3−C4−C5, C8−C9−C10, and C9−C10−C11 bonds angles are the smallest (173(2)°−174(2)°). The ξ value (0.03378) is somewhat higher than for the tetraynes with similar conformations.

The unsymmetrically substituted complexes C8-**15**, C8-**22**, C8-**23**·CH_2Cl_2, and C10-**3** adopt unsymmetric bow conformations **C**, with ξ values of 0.16750, 0.15396, 0.04936, and 0.08129. The first, which has the highest ξ value, is depicted in Figure 10. The lower homologue of C8-**15**, a 1,3,5-hexatriyne, is similarly distorted,[31] with a ξ value of 0.15842. The related unsymmetrical rhenium tetrayne C8-**14** is harder to classify. It has a higher degree of linearity (ξ 0.05519) and is perhaps best regarded as an unsymmetric S-shaped or random conformation (**F**). The rhenium fragment in C8-**14** and C8-**15** is a strong "single face" π donor, and the chain conformations were closely examined for possible electronic effects. For example, some zwitterionic vinylidene or $^{+}Re{=}C{=}CR^{-}$ character would have predictable geometric consequences.[31] However, no such influence was apparent.

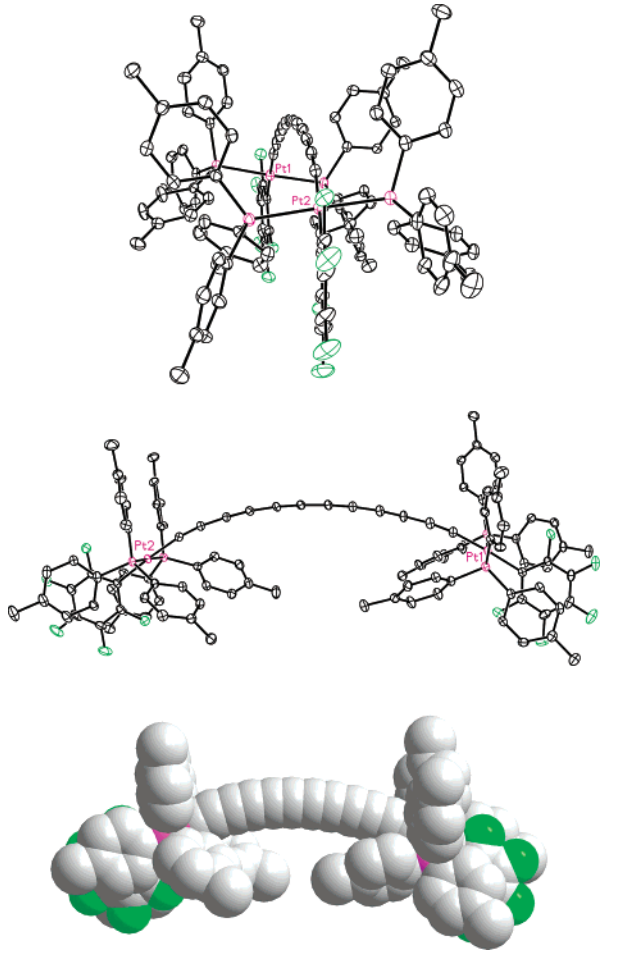

Figure 8. Carbon chain conformation in C12-**5**·4C_6H_6·EtOH (**B**, symmetric bow).

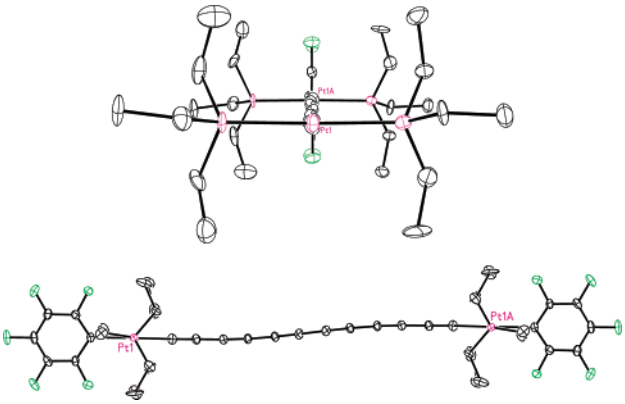

Figure 9. Carbon chain conformation in C12-**8** (**D**, kinked; top: with C_6F_5 ligands omitted).

Several of the diplatinum complexes in Charts 3 and 6 exhibit S-shaped conformations **E**. One good example is the hexayne C12-**4**·2C_6H_6. This centrosymmetric structure, which is shown in Figure 11, gives a ξ value of 0.06208. The X−C1−C2 and C1−C2−C3 bond angles (174.0(3)°, 174.5(4)°) are much lower than the others (177.5(4)°−178.9(6)°). Additional examples include the tetraynes C8-**20**·

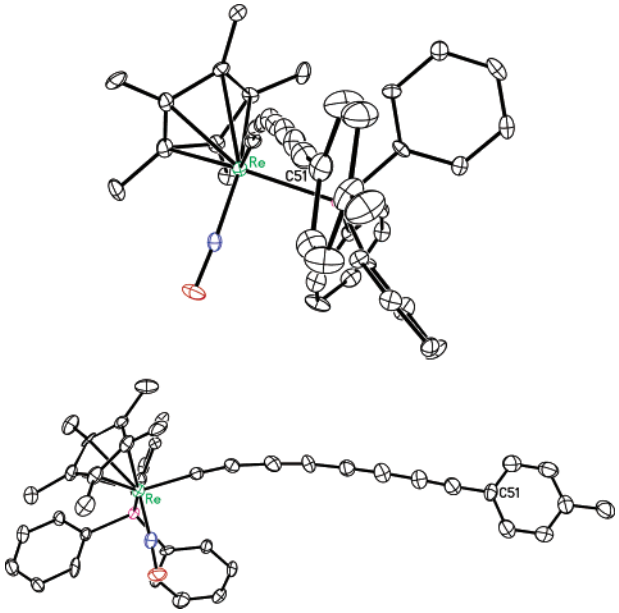

Figure 10. Carbon chain conformation in C8-**15** (**C**, unsymmetric bow).

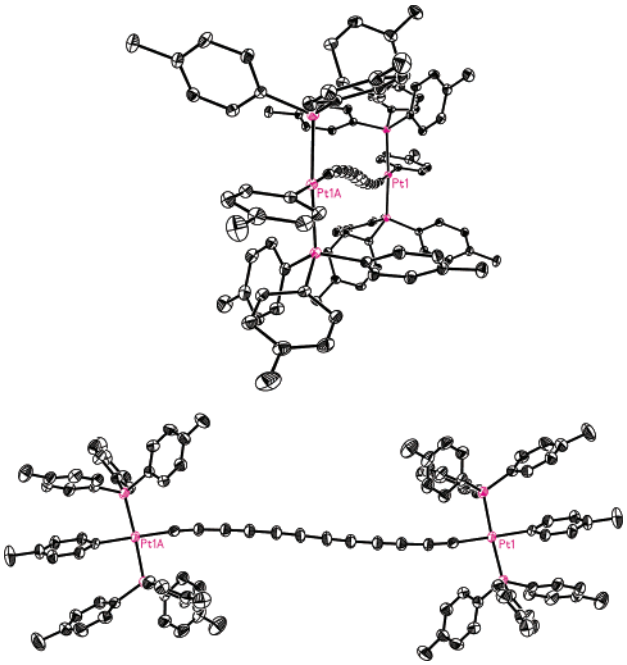

Figure 11. Carbon chain conformation in C12-**4**·2C_6H_6 (**E**, S-shaped).

4acetone·0.5$C_6H_4F_2$, C8-**21**·C_7H_8, and C8-**24**·EtOH, but their curvatures are less pronounced, as reflected by the ξ values (0.01564, 0.01785, 0.02386). The S-shape of tetrayne C8-**25**·acetone is in turn somewhat more distinct (ξ 0.04174). In contrast, the dicationic complex C8-**27**·4acetone is quite linear (ξ 0.01234). The one octayne, diplatinum complex C16-**1**·10C_6H_6, also exhibits a distinct S-shaped conformation (ξ 0.05602).

Two tetraynes, C8-**17** and C8-**26**, exhibit what can be regarded as extended S-conformations. Each contains a 20-atom chain consisting of two metals and sixteen sp carbons. This entire assembly defines an S-shape, as illustrated for the latter in Figure 12. In principle, ξ values can be calculated for the twenty atom chains. However, the quality of these structures

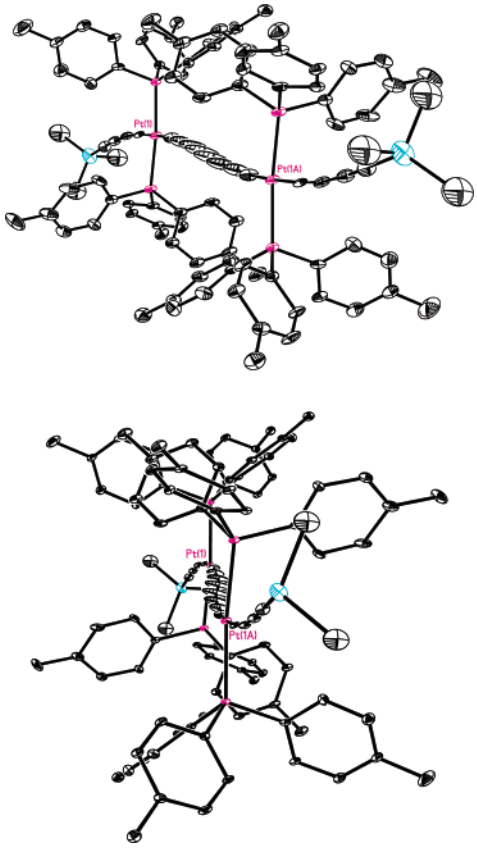

Figure 12. Carbon chain conformation in C8-**26** (**E**, extended S-shaped).

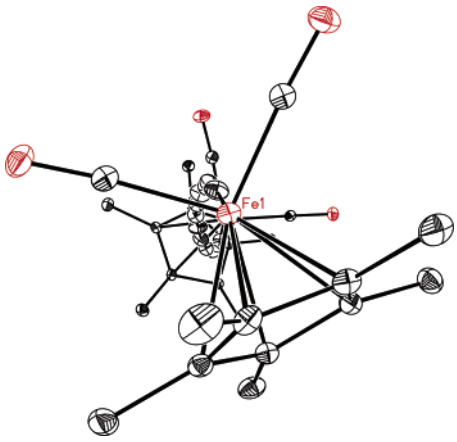

Figure 13. Carbon chain conformation in C12-**3** (**E**, S-shaped with secondary spiral).

is outside the range set for quantitative comparisons. When C8-**26** is viewed end-on, a slight secondary spiral motif is also evident (Figure 12, bottom).

The structure of the diiron hexayne C12-**3** is of high quality, and also exhibits a S-shaped conformation **E** with a spiral motif. This is highlighted in Figure 13. This compound gives the highest ξ value of all those with S-shaped conformations (0.12778). The secondary mode of distortion is undoubtedly a contributing factor. Interestingly, C12-**3** is one of the few S-shaped polyynes that are not centrosymmetric (the others are from Chart 4 as described below). The only other compound from Charts 2, 3, or 6 with an S-shaped conformation is the ferrocenyl-containing tetrayne C8-**18** (ξ 0.02835).

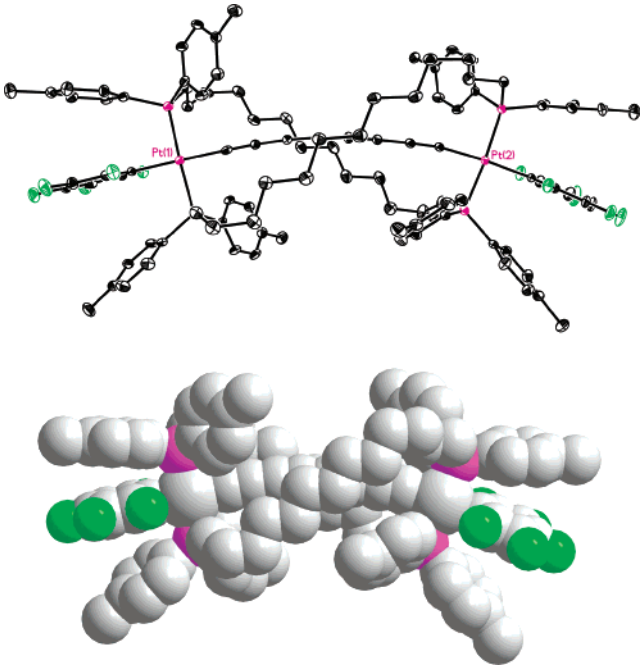

Figure 14. Carbon chain conformation in C8-**30** (**B**, symmetric bow).

The four diplatinum tetraynes in Chart 4 contain two additional bridges between the endgroups. Since different solvates can be crystallized, they correspond to seven structures (Table 3), of which only C8-**31**·$2C_7H_8$ is centrosymmetric. Most exhibit a bow conformation of some type, and four are among the least linear, as noted in the previous section (C8-**29**·$1.5C_6H_6$, C8-**29**·$1.5C_7H_8$, C8-**30**, C8-**32**·$2CHCl_3$; ξ 0.15694, 0.13900, 0.17226, 0.21115). The first two of these, C8-**29**·$1.5C_6H_6$ and C8-**29**·$1.5C_7H_8$, feature unsymmetric bow conformations (**C**). Note here that the Pt−C1−C2 and C7−C8−Pt′ angles in Table 3 are very different (171.7(3)° vs 178.0(3)° and 175.9(5)° vs 171.6(4)°). We believe that the second two compounds, C8-**30** (Figure 14) and C8-**32**·$2CHCl_3$, are best regarded as symmetric bows (**B**), despite the similar bond angle anisotropy in the former. For some reason, this structure appears by eye more symmetric.

Complex C8-**31**·$5.5C_7H_8$ was included among the four "essentially linear" molecules above (ξ 0.03634; average bond angle 179.1°, lowest bond angle 178.3(5)°). However, upon close visual inspection, a very slight symmetric bow is evident. The solvate C8-**31**·$2C_7H_8$ exhibits a mildly S-shaped conformation (**E**). Note that although the average bond angle (177.4°) is further from 180° than C8-**31**·$5.5C_7H_8$, the ξ value indicates a higher degree of linearity (0.03096)—a logical consequence of the inflection point. Complex C8-**32**·$4C_7H_8$ also exhibits a mildly S-shaped conformation, with a very similar average bond angle (177.7°) and ξ value (0.02825). The related hexayne C12-**9** contains two independent molecules in the unit cell, both of which exhibit S-shaped conformations. However, quality of the data lie outside the limits set for quantitative comparisons.

One general comment about chain conformation is best made in retrospect. The nanotechnology boom has prompted comparisons between certain types of molecules and a variety of macroscopic objects such as motors, windmills, and trucks. In the same vein, it is tempting to view the various chain conformations as "frozen quantum vibrational states". For example, the S-shaped conformation **E** would represent a higher energy mode than the symmetric bow conformation **B**. Still higher energy modes would approach linearity. The spiraling seen in some structures would constitute another possible quantized property with different energy levels. Conceptually related rod-bending modes of [*n*]staffanes have been predicted computationally to appear in the far IR (160−35 cm^{-1}) but have not yet been observed.[52]

8. Classification of Packing Motifs

Tables 1−4 and S1 (Supporting Information) show that, as would be expected, 1,3,5,7-tetraynes and higher homologues crystallize in a number of space groups. In the present sampling (46 crystal modifications that give 48 independent structures), three appear with particular frequency: $P\bar{1}$, 16 crystal modifications or 35%; $P2_1/c$, 11 crystal modifications or 24%, $P2_1/n$, 8 crystal modifications or 17%. The last is a nonstandard space group, and such structures are more rigorously solved in $P2_1/c$ (41% together). The natural statistical abundances of standard space groups are well-known.[53] The groups $P\bar{1}$ and $P2_1/c$ (including $P2_1/n$) account for 14.26 and 35.29% of organic crystal classes, and 22.06 and 41.79% of nonorganic crystal classes (homomolecular crystals without solvates; 21.06 and 25.84% or 30.73 and 36.34% when solvates are present). Hence, no pronounced skewing of the macroscopic statistical distribution is obvious.

Just as certain space groups dominate, so do certain chain packing patterns. First, all crystal structures exhibit sets of parallel chains or X/X′ vectors. In many, including all of the space group $P\bar{1}$, all chains or vectors are parallel. In others, as described below, there are two or more sets of parallel chains or vectors with a nonparallel relationship. We use the term "parallel chains" whenever the X/X′ vectors are parallel, even if the chain conformations introduce nonidealities. For example, neighboring molecules with bow conformations can have parallel orientations, ((, and two limiting antiparallel orientations, ( ) and)(. Note that in a lattice consisting only of parallel chains, there are an infinite number of subsets that can be defined (horizontally between vertical stacks, diagonally between stacks, etc.). For this reason, the term "set" can be confusing. Although we try to avoid it, it cannot be completely eliminated.

The distance between the *closest* parallel chains in a lattice is of obvious interest. For this calculation, it would in theory be possible to use the X/X′ vectors or least squares lines. For simplicity, however, we use the distance between the two closest atoms (which are in all but one case carbon atoms). These and other data are summarized in Table 5. Contacts range from 3.486 Å for C8-**10** and 3.512 Å for C12-**7** to 11.985 Å for C8-**31**·$5.5C_7H_8$. The van der Waals radius of an sp carbon is 1.78 Å,[54] so the values for C8-**10** and C12-**7** are less than the sum of the van der Waals radii (3.56 Å). Six other compounds exhibit

Table 5. Packing Parameters for Polyynes

compound	chain−chain contact (parallel) (Å)[a]	ϕ (°)	offset distance (Å)	fractional offset	chain−chain contact (nonparallel) (Å)[a]	angle between nonparallel chains (°)
C8-**2**	3.853	53.5	3.52	0.28	3.593	61.8
C8-**3**	4.018	55.7	3.18	0.27	4.884	72.5
C8-**4**	4.490	25.8	9.01	0.77	6.564	47.4
C8-**6**·BU·C	5.125	42.1	5.22	0.44	5.390	6.1
C8-**7a**	3.636	27.9	6.82	0.58	6.312	55.7
C8-**7b**	7.824	72.4	2.46	0.21	9.358	40.2
C8-**8**	3.924	83.9	0.42	0.04		
C8-**9**	3.700	68.9	1.74	0.15		
C8-**10**	3.486	74.8	1.02	0.08	4.91	55.3
C8-**12**	5.325	25.6	9.97	0.85		
C8-**14**	7.783	−69.2	−2.89	−0.23	7.569	86.4
C8-**15**	5.088	43.2	6.14	0.50	8.841	84.8
C8-**18**	3.732	30.3	6.40	0.54	5.573	60.6
C8-**20**	8.890	61.1	4.93	0.38		
C8-**21**·C_7H_8	11.936	79.7	2.17	0.17	9.675	20.6
C8-**22**	5.538	−61.7	−3.45	−0.27		
C8-**23**·CH_2Cl_2	5.025	−29.5	−9.68	−0.76	8.078	61.0
C8-**24**·EtOH	9.222	44.5	9.63	0.74		
C8-**25**·acetone	8.764	54.2	6.56	0.51	13.109	78.3
C8-**27**·4acetone	4.201[b]	17.0	13.54	1.05	10.060	34.0
C8-**29**·1.5C_6H_6	8.070	65.5	4.45	0.35		
C8-**29**·1.5C_7H_8	7.974	63.0	4.85	0.38		
C8-**30**	9.340	59.9	6.17	0.49		
C8-**31**·2C_7H_8	11.433	44.8	11.27	0.88	11.539	85.0
C8-**31**·5.5C_7H_8	11.985	65.3	5.65	0.44		
C8-**32**·4C_7H_8	7.296	54.2	5.29	0.41	16.150	50.5
C8-**32**·2$CHCl_3$	7.780	82.5	1.26	0.10		
C10-**1**	3.645	44.2	3.74	0.26	5.431	88.4
C10-**3**	7.036	−77.3	−1.47	−0.13		
C12-**1**	5.050	21.7	12.49	0.70	5.844	43.3
C12-**3**	5.021	36.4	5.92	0.42	5.149	32.5
C12-**4**·2C_6H_6	7.884	43.4	8.09	0.45		
C12-**5**·4C_6H_6·EtOH	7.535	50.4	6.73	0.40	11.534	89.6
C12-**7**	3.512	29.3	6.40	0.38		
C12-**8**	5.353	23.0	13.21	0.73		
C16-**1**·10C_6H_6	8.786	29.2	14.62	0.63		

[a] Shortest carbon−carbon distance between parallel polyyne chains as described in the text, unless noted. [b] Pt−Pt distance. The shortest carbon−carbon distance for C8-**27**·4acetone is 6.111 Å.

chain−chain distances of less than 4.0 Å (C8-**2**, C8-**7a**, C8-**8**, C8-**9**, C8-**18**, C10-**1**). All except C8-**10** and C8-**2** feature aryl or alkenyl endgroups (i.e., sp^2 hybridized termini). The 16 compounds in Table 5 with *two* bulky platinum endgroups (C8-**20**·4acetone ·0.5$C_6H_4F_2$, C8-**21**·C_7H_8, C8-**24**·EtOH through C8-**32**·2$CHCl_3$, C12-**4**·2C_6H_6, C12-**5**·4C_6H_6·EtOH, C12-**8**, C16-**1**·10C_6H_6) exhibit an average chain-chain distance (9.05 Å) much greater than that of the 18 compounds without a platinum endgroup (4.90 Å).

The closest parallel chains will furthermore be characterized by a "translation" or "offset", which is easily visualized with reference to a brick wall. As shown in Figure 15, one extreme (**J**) would have no (zero) offset between layers, giving a "ladder motif". The other extreme (**K**) would have an offset of a half-brick, i.e., "maximally staggered". In the macroscopic physical world, the former pattern is much weaker mechanically. Even in these politically correct times, anyone erecting such a wall would be the subject of cruel ethnic jokes. However, as will be seen below, this limit is not entirely avoided by the building blocks in Charts 1−6. Additional types of two-dimensional networks possible with square or rectangular bricks have been reviewed elsewhere.[19]

Of course, the building blocks in Charts 1−6 are not bricks. Several are quite rodlike, sometimes with "flat" aryl endgroups, but most are better approximated as dumbbells. Various limits for walls or arrays constructed of such objects are illustrated in Figure 15. One extreme is again a "ladder motif" (**L**), which enforces a minimum layer separation. Note the gaps between dumbbells along the horizontal axes. These interstices, which are necessary to generalize this analysis, can be occupied by solvate molecules or additional sets of parallel chains (i.e., perpendicular or angular running). Of the 46 crystal modifications in Tables 1−4 and S1, 18 incorporate solvent or guests.

Another limit would be to translate adjacent layers just enough for the head of one dumbbell to slip past its partner in the adjacent layer (**M**). Another is attained when the head of one is translated to the midpoint of the handle of its partner in the adjacent layer (**N**). Yet another involves a further translation such that the heads in adjacent layers are again slipped just past each other (**O**). Without the gaps between dumbbells along the horizontal axes, **M** and **O** would be equivalent. Relative to **L**, limits **M**−**O** allow the possibility of layer/layer intercalation and shorter chain−chain distances. However, since none of the crystal lattices show this phenomenon, the layer−layer distances are kept constant in Figure 15. Continuing the translational motion of adjacent

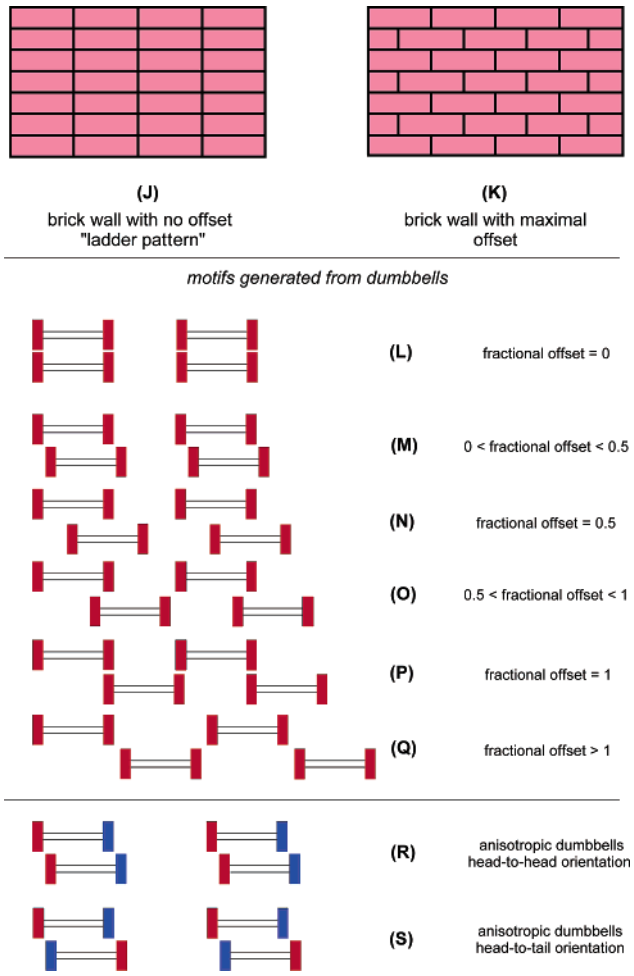

Figure 15. Some limiting packing motifs for parallel chains in two dimensions.

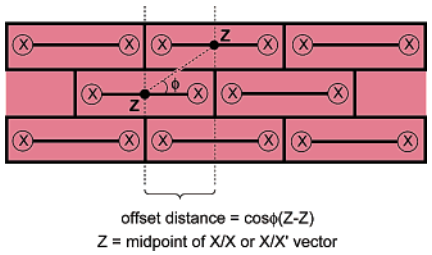

Figure 16. Derivation of key packing parameters for Table 5.

layers leads to the limit **P**. In the series **L**−**P**, the gaps between dumbbells along the horizontal axes are equal to the handle lengths. If the gaps are further increased, **P** is replaced by the array **Q**.

The translation or offset between parallel sp carbon chains has been previously analyzed for crystalline 1,3-butadiynes.[21,55] Under favorable geometric circumstances, these undergo topochemical polymerization, a subject treated below. As illustrated in Figure 16, we employ an equivalent treatment. We begin with the X/X′ vectors of neighboring chains, which are easier to visualize than the least squares lines used for the ξ values. The midpoints are identified, and a line drawn between them. The angle defined by this line and the X/X′ vector is termed ϕ, by analogy to the 1,3-butadiyne analyses.[56]

In the absence of translation or offset (**J** in Figure 15), ϕ is equal to 90°. In a wall consisting of maximally staggered square bricks (similar to **K**), ϕ would be 45°. In a wall consisting of maximally staggered long slender bricks, ϕ can be much less than 45°. In arrays such as **O**−**Q**, with gaps between dumbbells along the vertical axes, ϕ can also be much less than 45°. As summarized in Table 5, the values obtained range from highs of 83.9° (C8-**8**) and 82.5 (C8-**32**·2$CHCl_3$) to lows of 17.0° (C8-**27**·4acetone), 21.7° (C12-**1**), and 23.0° (C12-**8**). In accord with the analogy to long slender bricks, the average ϕ value for the pentaynes, hexaynes, and octaynes in Table 5 (40.04) is much lower than that for the tetraynes (52.90).

Another factor plays a role in the ϕ values. When the bricks or dumbbells are anisotropic, as is the case for noncentrosymmetric molecules, the offset has directionality. Both parallel and antiparallel arrangements are possible, as illustrated with color anisotropy by **R** and **S** in Figure 15. In the absence of color, both are equivalent to **M**. To differentiate lattices with antiparallel arrangements **S**, negative ϕ values are employed. Given the high degree of symmetry for most of the polyynes with like endgroups, this distinction is only applied in the present analysis to the five polyynes with unlike endgroups. As summarized in Table 5, C8-**15** gives a positive ϕ value, whereas C8-**14**, C8-**22**, C8-**23**·CH_2Cl_2, and C10-**3** give negative ϕ values. Thus, for the last four compounds, the bulky metal-containing endgroups of one molecule are paired with the smaller organic endgroups of the partner molecule in the closest parallel chain.

The ϕ values can in turn be used to express the translation or offset in angstroms (distance between the midpoints of parallel chains multiplied by cos ϕ). These values are also incorporated into Table 5, with negative values for antiparallel cases as discussed in the preceding paragraph.[56] As would be intuitively expected, longer chains tend to yield greater offset distances (average for tetraynes and pentaynes: 5.32 Å; average for hexaynes and octaynes, 9.63 Å). Given this dependence, and the conceptually similar dependence of ϕ on chain/chain spacings, a normalized parameter is desirable. Accordingly, we divide the offset by the X/X′ distance and term the resulting dimensionless number "fractional offset". Values are summarized in Table 5. For calibration, note that the idealized arrays **L**−**Q** in Figure 15 have fractional offsets in the following ranges: **L**, 0; **M**, > 0 and < 0.5; **N**, 0.5; **O**, > 0.5 and < 1.0; **P**, 1.0; **Q**, > 1.0.

Twelve molecules have fractional offset values greater than 0.5, or "half a chain length": C8-**4**, C8-**7a**, C8-**12**, C8-**18**, C8-**23**·CH_2Cl_2, C8-**24**·EtOH, C8-**25**·acetone, C8-**27**·4acetone, C8-**31**·2C_7H_8, C12-**1**, C12-**8**, and C16-**1**·10C_6H_6. In all cases except C8-**23**·CH_2Cl_2, the endgroups are identical. Some feature svelte aryl or sp^2 moieties (C8-**4**, C8-**7a**), others zaftig ferrocenyl-containing moieties (C8-**10**, C8-**18**), others bulky platinum moieties (C8-**23**·CH_2Cl_2, C8-**24**·EtOH, C8-**25**·acetone, C8-**27**·4acetone, C8-**31**·2C_7H_8, C12-**8**, C16-**1**·10C_6H_6), and still others trialkylsilyl groups (C12-**1**, C8-**23**·CH_2Cl_2). Hence, there is no

obvious correlation with structure. The greatest fractional offset, 1.05, occurs in C8-**27**·4acetone. This value minimizes the distance between positively charged platinum endgroups in neighboring chains (4.201 Å), which would seemingly be electrostatically unfavorable. However, there may be compensating interactions as analyzed below.

The lowest fractional offset value is found with C8-**8** (0.04; 0.42 Å). This "brick wall" motif is analyzed further below. Intuitively, the bulkiest endgroups might have been expected to exhibit fractional offset values close to 0.5, corresponding to the dumbbell array **N** ("maximally nested"). Most of the seven structures with fractional offset values of 0.44−0.54 feature endgroups that can be regarded as bulky (C8-**6**·BU·C, C8-**15**, C8-**18**, C8-**25**·acetone, C8-**30**, C8-**31**·$5.5C_7H_8$, C12-**4**·$2C_6H_6$). Nonetheless, there are many structures with equally bulky endgroups that are far outside this range. Also, plots of fractional offset values as a function of chain−chain distance are essentially random, with no obvious trends or relationships.

In many crystals, including all with the space groups $P2_1/c$ and $P2_1/n$, there are two *non-parallel* sets of parallel chains. Although each set of parallel chains is characterized by an offset, these are in all cases equal. The distances or closest contacts between the two sets of chains can be calculated as outlined above for parallel chains, and are summarized in Table 2 ("chain−chain contact (nonparallel)"). As will be illustrated below, these distances are sometimes less than those between parallel chains. The angles defined by the two sets of chains are calculated from the X/X′ vectors using SHELXLS. These range from 89.6° to 6.1°, with an average of 57.7° (Table 2). Finally, two crystals, C8-**2** and C8-**3**, both in space group *Pbcn*, contain four nonparallel sets of parallel chains, all with equal offset. The closest contacts are similarly noted in Table 5.

9. Packing Motifs: Specific Examples

In this section, the phenomena described in the previous section are illustrated with specific packing diagrams.

9.1. The tetrayne C8-**8**, with flat *o*-bromophenyl endgroups, crystallizes in the space group $P1$ ($Z = 2$). As depicted in Figure 17, all chains are clearly parallel. Aryl/aryl π stacking interactions and bromine/bromine nonbonded contacts are evident, and these correspond to the closest chain−chain distances. The separation, 3.924 Å (C7C−C7E, C8C−C8E, etc.), is slightly greater than the sum of the van der Waals radii (3.56 Å). The fractional offset, 0.04, is the smallest in Table 5 (offset distance 0.42 Å), and the offset angle ϕ, 83.9°, is the largest. Hence, the closest parallel chains exhibit a "ladder" like packing (**J** or **L** in Figure 15). Compound C8-**8** is virtually unique in this regard, presumably due to the aryl/aryl π and bromine/bromine interactions. Directing effects due to halogen/halogen nonbonded contacts are well-known in crystal engineering.[57] The next lowest fractional offset values, 0.08, 0.10, and 0.15, are found for the ditellurium compound C8-**10** and diplatinum

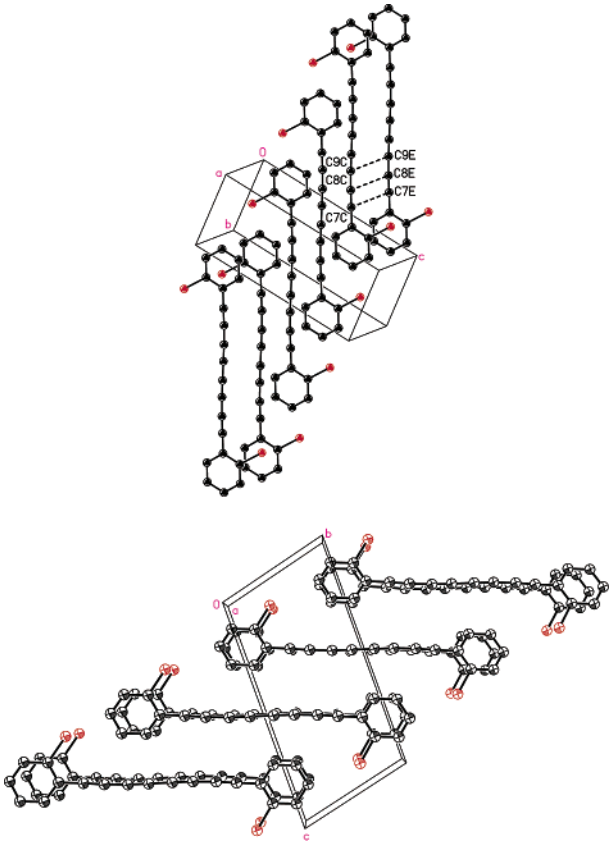

Figure 17. Packing diagram for C8-**8**.

complexes C8-**32**·$2CHCl_3$ and C8-**9**, all of which are analyzed below.

Of course, many nonnearest-neighbor subsets of parallel chains in C8-**8** can be defined. For example, molecules from different π stacks can be considered. The closest contacts in this dimension, illustrated in the bottom view in Figure 17, are 4.098 Å. Such subsets will be characterized by different offset quantities. The stacks in the bottom view exhibit a brick-wall motif (**K** or **N** in Figure 15), with fractional offsets of 0.61.

9.2. The pentayne C10-**1** can be derived by removing the bromine atoms from C8-**8** and inserting an additional C≡C linkage. Now the molecule crystallizes in a dramatically different motif and in the space group $P2_1/n$ ($Z = 2$). As depicted in Figure 18, two *nonparallel* sets of parallel chains are evident. The closest distance between parallel chains, 3.645 Å (C4B−C1G), is one of the three smallest in Table 5. It is barely larger than the sum of the van der Waals radii, as illustrated in the bottom view in Figure 18. The fractional offset is 0.26 (offset distance 3.74 Å), which completely removes the aryl/aryl π stacks found in C8-**8**.

As in C8-**8**, there are nonnearest-neighbor subsets of parallel chains with different offset values. This universal feature will not be commented upon again. The closest contact between the two nonparallel sets of parallel chains is 5.431 Å (C1D−C2B). The sets define an angle of 88.4°, as accurately represented in Figure 18. Other perspectives can distort this relationship (much as the end-on views of the chains in section 7). In any event, the two sets of chains define a classic herringbone pattern.

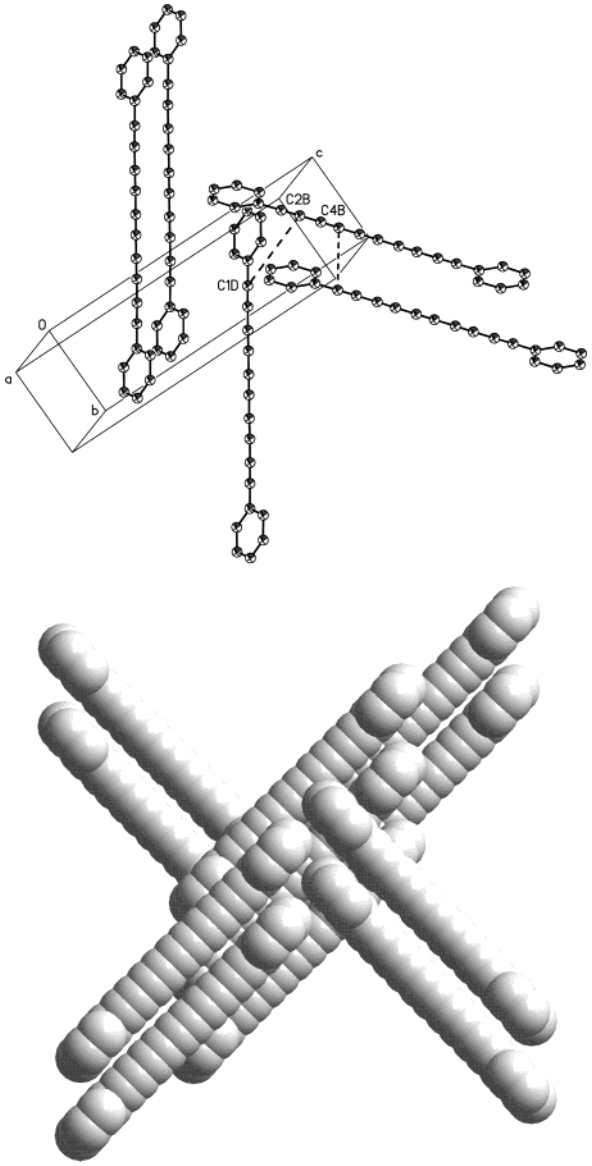

Figure 18. Packing diagram for C10-**1**.

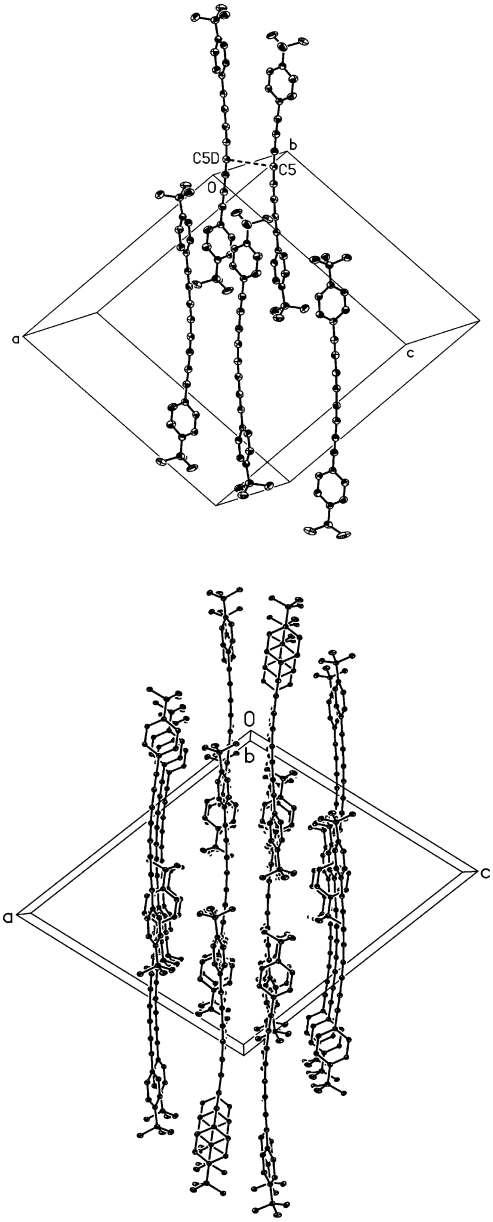

Figure 19. Packing diagram for C8-**9**.

9.3. The tetrayne C8-**9** can be derived by removing the bromine atoms from C8-**8** and introducing *p*-(*tert*-butyl) groups. This moderate perturbation again dramatically affects the packing motif. Compound C8-**9** crystallizes in the space group *I*2/*a* ($Z = 8$). As shown in Figure 19, all chains are parallel, with a closest distance of 3.700 Å (C5−C5D). This is only slightly greater than in C10-**1**, which lacks the *p*-(*tert*-butyl) substituent. As noted above, the aryl termini are not coplanar, precluding aryl/aryl π stacking between nearest neighbors. However, π stacking between nonnearest neighbors is evident in the bottom view. The small fractional offset between nearest parallel chains, 0.15 (offset distance 1.74 Å), appears to preserve some type of aryl/aryl interaction (possibly an attractive edge/face of CH/π relationship).[58]

9.4. The tetrayne C8-**7** gives the only true polymorphs found in higher polyynes to date, C8-**7a** and C8-**7b**. The former crystallizes in the space group $P2_1/c$ ($Z = 4$), and the latter in $P2_1/n$ ($Z = 2$). The bond lengths are almost identical, and the angles differ only slightly (largest deviation, 1.8° for X−C1−C2). As shown in Figure 20, C8-**7a** exhibits a much higher fractional offset value (0.58; offset distance 6.82 Å) than C8-**7b** (0.21; offset distance 2.46 Å). The endgroups in C8-**7a** can therefore better nest in the middle of the chains of the nearest neighbors. Accordingly, the closest chain−chain distance is only 3.636 Å in C8-**7a** (C5−C10B), but 7.824 Å in C8-**7b** (C8E−C7G). As would be expected, the crystal density of C8-**7a** is also higher (1.018 vs 0.993 g/cm^3).

9.5. The adamantyl-substituted tetrayne in C8-**6**·BU·C is the most dumbbell-like of the purely organic molecules. It crystallizes in the space group $P2_1/n$ ($Z = 4$), as shown in Figure 21. There are two nonparallel sets of parallel chains. However, the angle between them is only 6.1°, which is the lowest in Table 5 (average value 57.7°) and makes them difficult to visually distinguish. The fractional offset, 0.44 (offset distance 5.22 Å), is close to the limit that would be intuitively expected for dumbbell-shaped molecules (0.50). As illustrated in Figure 21, the closest carbon−carbon contacts are similar in every direction (nearest

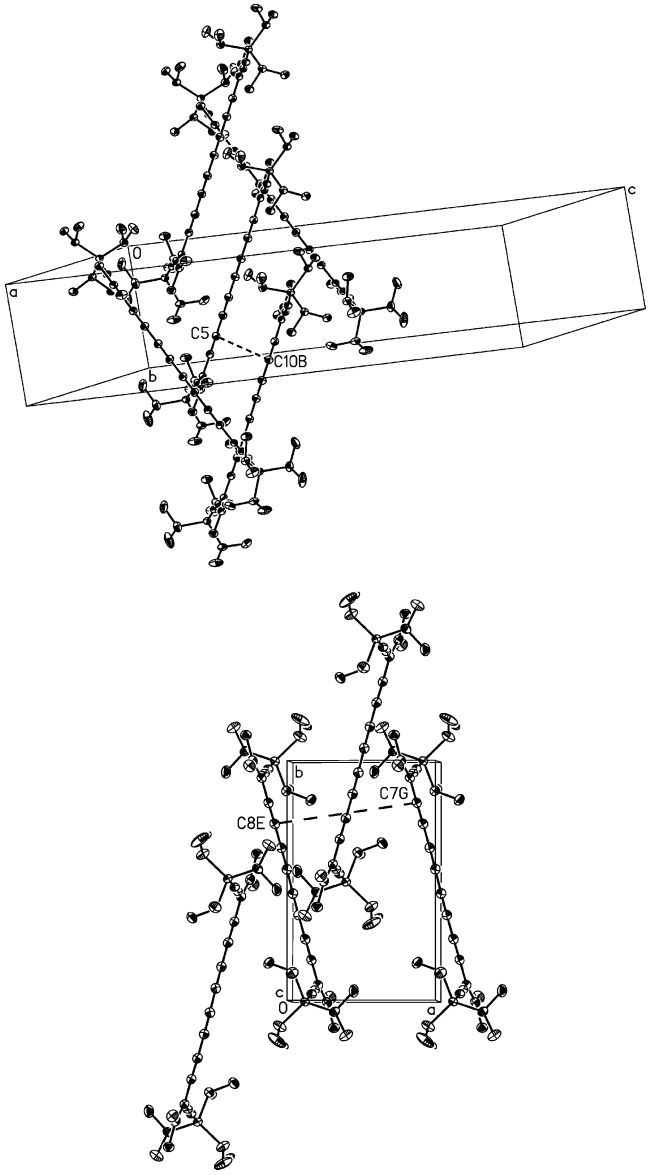

Figure 20. Packing diagrams for C8-**7a** (top) and C8-**7b** (bottom).

parallel chain, 5.125 Å (C15−C18E) and 5.150 Å (C16−C17E); nearest nonparallel chain, 5.390 Å (C11−C18G); next-nearest parallel chain, 5.553 Å (C11−C14D)), suggesting efficient packing.

9.6. The chiral monorhenium complex C8-**14** is one of several with unlike endgroups. The unit cell ($P2_1/n$) contains four molecules in paired, nearly orthogonal orientations, as shown in Figure 22. These propagate as two nonparallel sets of parallel chains throughout the lattice. The unsymmetrical monorhenium complex C8-**15** and monoplatinum complex C8-**23**·CH_2Cl_2 are analogous ($P2_1/n$, $Z = 4$). In contrast, the monoplatinum complex C8-**22** crystallizes with all chains parallel ($P\bar{1}$, $Z = 2$). Figure 22 further shows that the pairs have head-to-tail arrangements, and opposite absolute configurations at rhenium. In C8-**23**·CH_2Cl_2 and C8-**22**, the closest parallel chains also have head-to-tail arrangements, but in C8-**15** (illustrated in Figure 23) they do not.

The angles between the nonparallel sets of parallel chains in C8-**14**, C8-**15**, and C8-**23**·CH_2Cl_2 are 86.4°, 84.8°, and 61.0°. With appropriate perspectives,

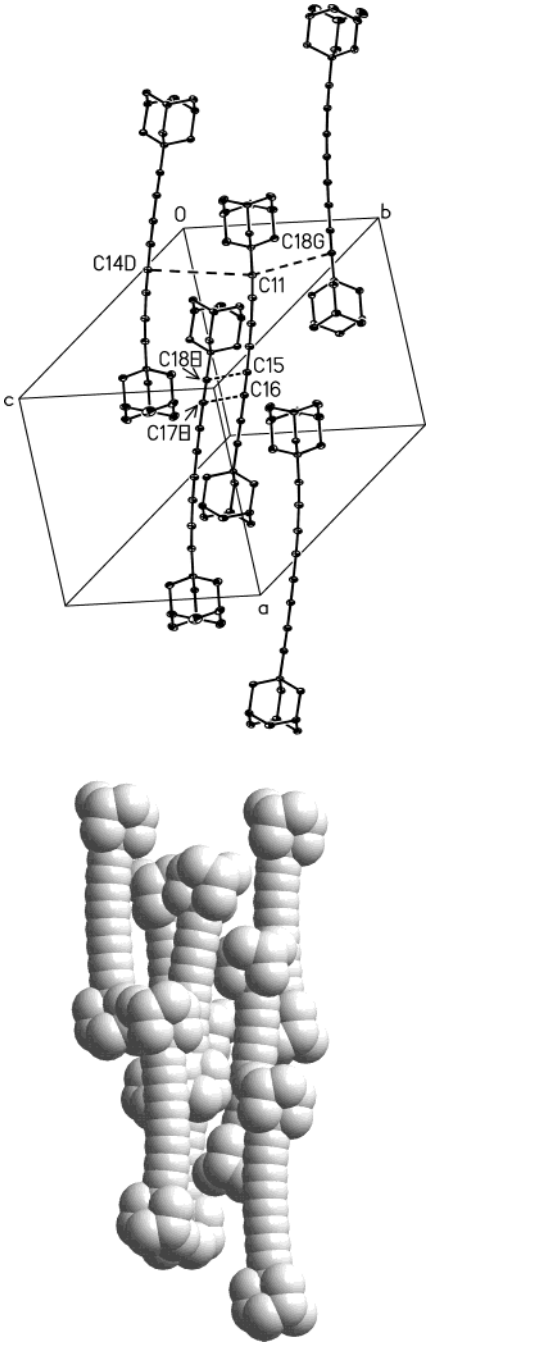

Figure 21. Packing diagram for C8-**6**·BU·C with guest molecules omitted.

"herringbone" or "zig-zag" motifs are apparent. Interestingly, the closest contact between nonparallel chains in C8-**14** (7.569 Å) is shorter than that between parallel chains (7.783 Å, C3−C8C). The fractional offset value for C8-**14**, −0.23 (offset distance −2.89 Å), is negative due to the head/tail relationship. Regardless, the absolute value is one of the smaller. The monoplatinum complexes C8-**23**·CH_2Cl_2 and C8-**22** are in most respects similar, with somewhat shorter distances between closest parallel chains (5.025 and 5.538 Å).

In C8-**15**, the closest contact between parallel chains (5.088 Å, C43B−C48D) is much shorter than that between nonparallel chains (8.841 Å). The fractional offset, 0.50 (offset distance 6.14 Å), is much higher than that of C8-**14**, and involves molecules of

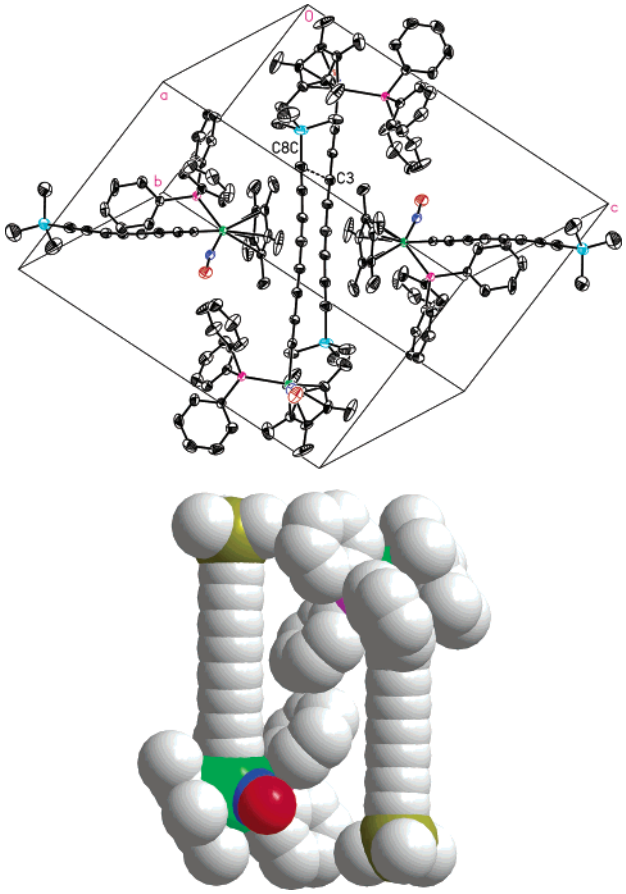

Figure 22. Packing diagram for C8-**14**.

identical chirality (left side of top perspective in Figure 23). The next-nearest parallel chains feature molecules of opposite chirality in head-to-tail arrangements (right side of top perspective). The bottom perspective in Figure 23 highlights other nonnearest sets of parallel chains, and provides a rationale for the marked (unsymmetric) bow conformation (ξ 0.16750). In each case, the carbon chains curve away from the phenyl rings of a stack of PPh_3 ligands, and toward a complementary stack of chains. The *p*-tolyl endgroups of the two stacks are in close proximity, and define approximately parallel planes separated by 3.0−3.5 Å. The *p*-tolyl groups are in even closer proximity to the terminal C≡C linkages of the complementary chains. In any event, some type of π/π interaction is implicated.

9.7. Compound C8-**20**·4acetone·0.5$C_6H_4F_2$ is one of the simpler diplatinum complexes with regard to packing motif. It crystallizes in the space group $P\bar{1}$, which requires all chains to be parallel. Unlike C8-**8** above, it contains only one molecule per unit cell (Z = 1). The molecules are quite evenly distributed in all dimensions of crystal space. As shown in Figure 24, the closest contact between parallel chains is 8.890 Å (C3AA−C2C). The next-nearest parallel chain is only slightly further removed (9.279 Å). The fractional offset, 0.38 (offset distance 4.93 Å), is not far from the 0.50 of idealized array **N** (Figure 15). However, as noted above, the diplatinum complexes span a large range of fractional offset values.

A view along the *b* axis of C8-**20**·4acetone·0.5$C_6H_4F_2$ reveals an aesthetically pleasing pattern, as shown

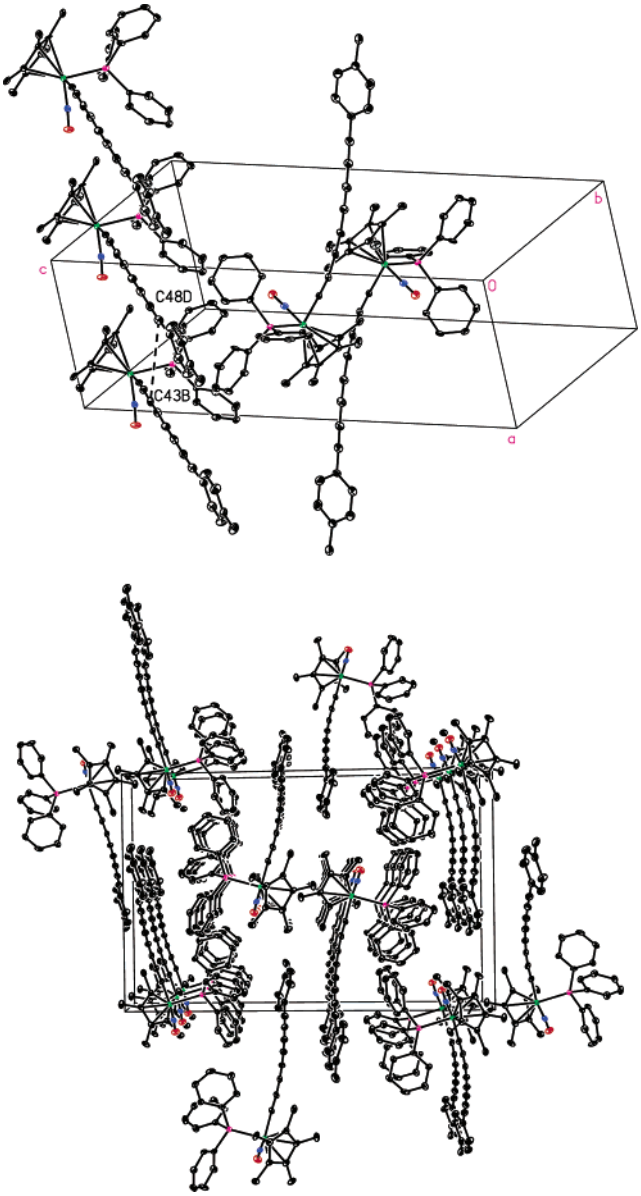

Figure 23. Packing diagram for C8-**15**.

in the bottom view in Figure 25. Importantly, the carbon chains do not lie in the plane of the paper, as required for a wall-like motif (e.g., **K** in Figure 15). The closest parallel chains are contained in the approximately vertical stacks. Many of the other polyynes can be displayed similarly.

9.8. In C8-**21**·C_7H_8, the *p*-tolyl endgroups of C8-**20**·4acetone·0.5$C_6H_4F_2$ have been switched to pentafluorophenyl, the phenyl groups of the phosphine ligand have been switched to *p*-tolyl, and the solvate molecules altered. The compound now crystallizes centrosymmetrically in the space group $P2_1/c$ (Z = 2). As shown in Figure 25, there are two nonparallel sets of parallel chains that define an angle of 20.6°. The closest distance between parallel chains is 11.936 Å (C3B−C4A), and it is tempting to ascribe much of the increase versus C8-**20**·4acetone·0.5$C_6H_4F_2$ to the *p*-tolyl groups of the phosphine ligands (note how *p*-methyl substituents would lead to interactions in all of the views in Figure 24). The closest contact between nonparallel chains is shorter (9.675 Å). The fractional offset, 0.17 (offset distance 2.17 Å), is less

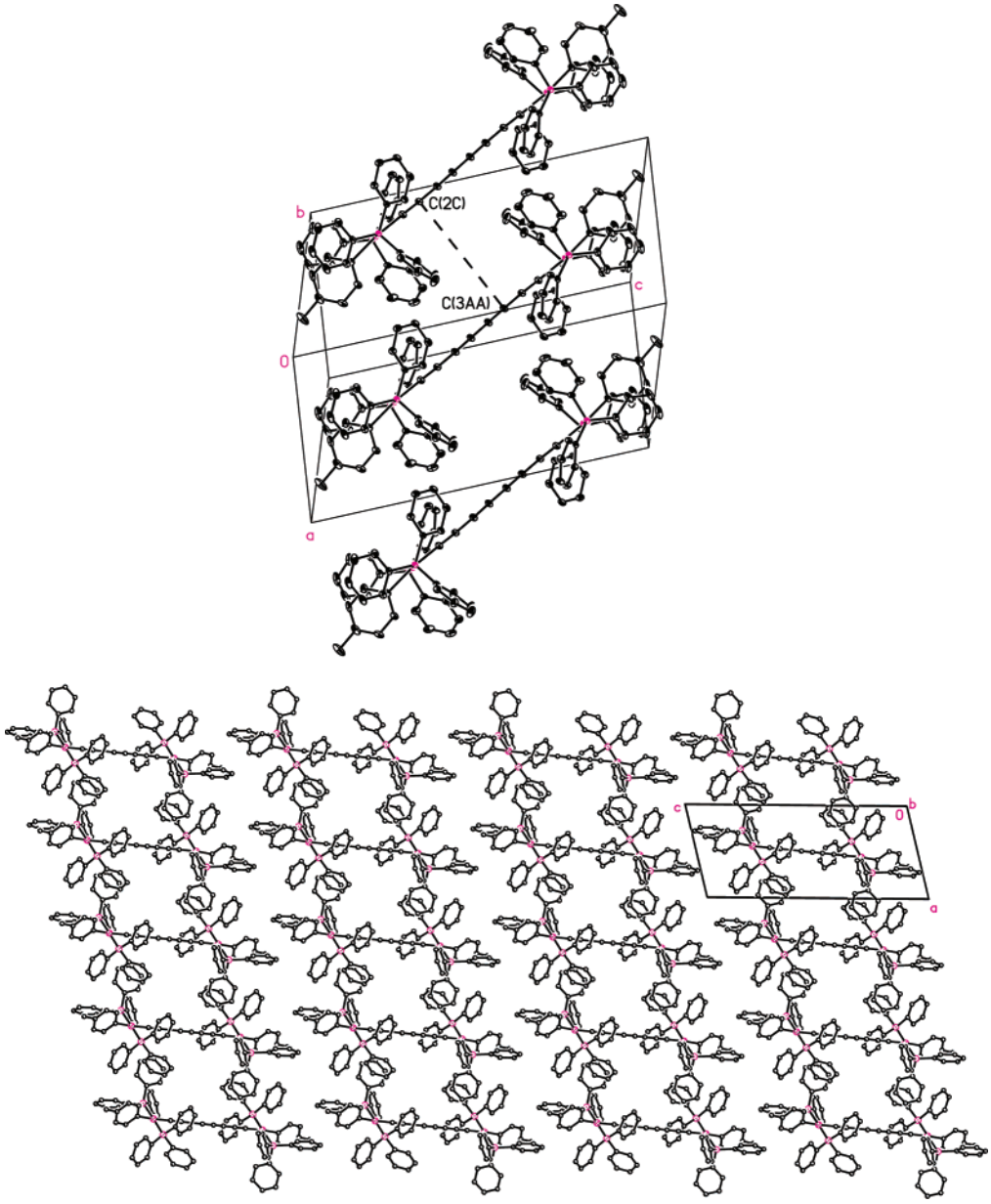

Figure 24. Packing diagram for C8-**20**·4acetone·0.5$C_6H_4F_2$ with solvent molecules omitted.

than half that of C8-**20**·4acetone·0.5$C_6H_4F_2$ and one of the smaller in Table 5.

9.9. In C8-**24**·EtOH, the major change is the replacement of a *p*-tolyl group on each phosphorus atom of C8-**21**·C_7H_8 by an aliphatic chain that bridges to the *trans*-phosphorus atom. The complex crystallizes in $P\bar{1}$ ($Z = 1$) with all chains parallel as illustrated in Figure 26. Although the representation of C8-**24** in Chart 3 gives the impression of a bulky endgroup, it should be kept in mind that the aliphatic chain is flexible. Thus, the closest contact between parallel chains (9.222 Å, C1A−C1B) is similar to that in C8-**20**·4acetone·0.5$C_6H_4F_2$. However, the fractional offset, 0.74 (offset distance 9.63 Å), is much higher. The next-nearest parallel chains (closest contacts 10.830 Å) have lower offset values (0.18, 2.39 Å). Interestingly, the aliphatic chains shield complementary sides of the sp carbon chain in a "half-clamshell" motif.

9.10. The diplatinum complex C8-**25**·acetone can be viewed as a structural perturbation of C8-**21**·C_7H_8. The pentafluorophenyl ligands have been changed to chloride ligands, and the solvent molecule switched. The complex again crystallizes in $P2_1/c$ ($Z = 2$). As shown in Figure 27, there are two nonparallel sets of parallel chains that define an angle of significantly greater than that in C8-**21**·C_7H_8 (78.3° vs 20.6°). The closest contact between parallel chains is now shorter (8.764 Å) and nearer to that of the PPh_3 complex C8-**20**·4acetone·0.5$C_6H_4F_2$. The fractional offset, 0.51 (offset distance 6.56 Å), is greater than those of C8-**20**·4acetone·0.5$C_6H_4F_2$ and C8-**21**·C_7H_8.

9.11. Since the diplatinum complex C8-**27**·4acetone is dicationic, the crystal lattice ($P2_1/c$, $Z = 2$) contains anions that are somewhat analogous to the solvent guests in other structures. As can be seen in Figure 28, the closest parallel chains exhibit the largest fractional offset found to date, 1.05 (offset distance 13.54 Å), corresponding to the limit **Q** in Figure 15. When values become greater than 1.0, the closest carbon−carbon contacts (here 6.110 Å) are no longer good measures of chain−chain separation. In this

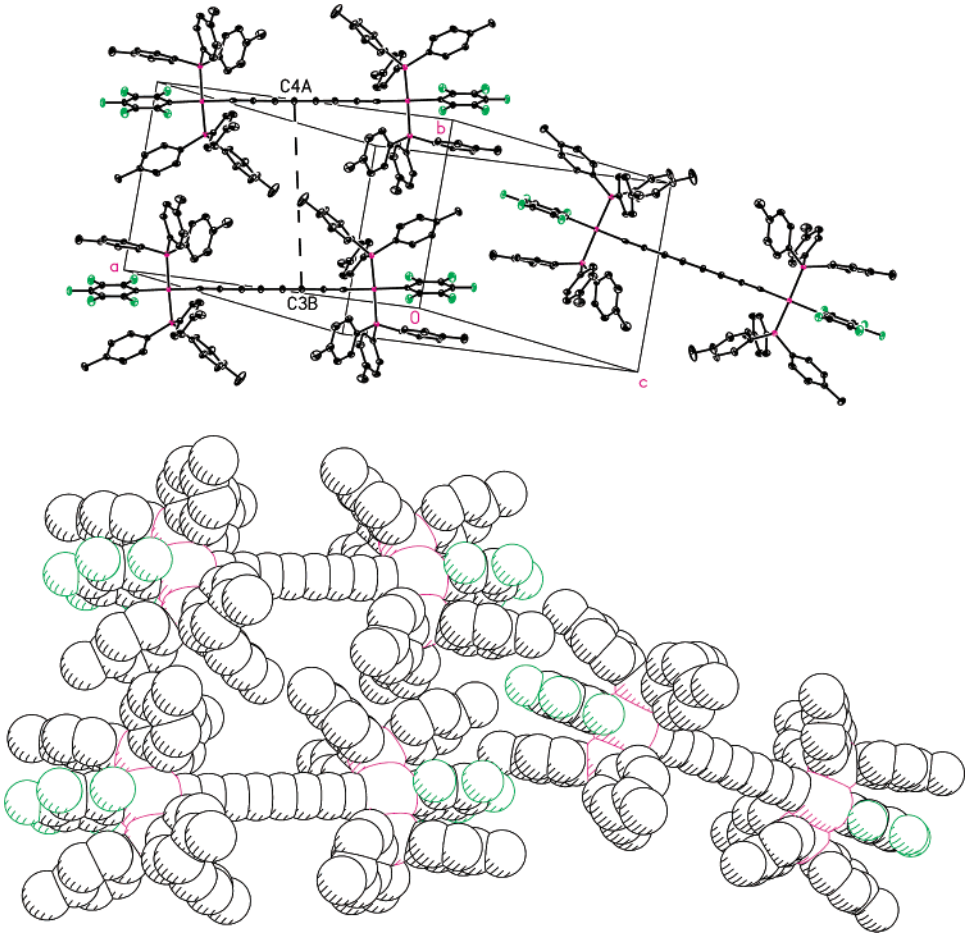

Figure 25. Packing diagram for C8-**21**·C_7H_8 with solvent molecules omitted.

case, the closest platinum−platinum contact, 4.201 Å, is an obvious substitute. Aryl/aryl π stacking interactions involving the outer pyridine rings of the tripyridal ligands are evident, and may represent a driving force for the large offset. The electronic configuration at platinum (d^8 or 16-valence-electron) is the same as in the other complexes. The lattice contains a nonparallel set of identical parallel chains that define an angle of 34° (closest contact 10.060 Å). These are represented in the middle column of the bottom perspective in Figure 28.

9.12. The diplatinum complexes in Chart 4, which contain diphosphine ligands that bridge the two platinum atoms, exhibit little in the way of new packing trends or phenomena. As summarized in Table 4, all crystallize in $P\bar{1}$, $P2_1/c$, or $P2_1/n$ space groups in motifs analogous to those described above. A representative packing diagram for a complex with only one set of parallel chains, C8-**29**·$1.5C_6H_6$, is given in Figure 29. The closest parallel chains have an antiparallel or)(curvature (ξ 0.15964), which illustrates a nonideality in our treatment. Namely, the closest carbon−carbon contact (8.070 Å) is somewhat less than the distance between the rigorously parallel X/X′ vectors. In contrast to C8-**15**, which also has a markedly curved chain (Figure 23), a careful inspection of the packing diagram reveals no obvious "single parameter rationalization" for the distortion. The same holds for the diplatinum complexes with still higher ξ values.

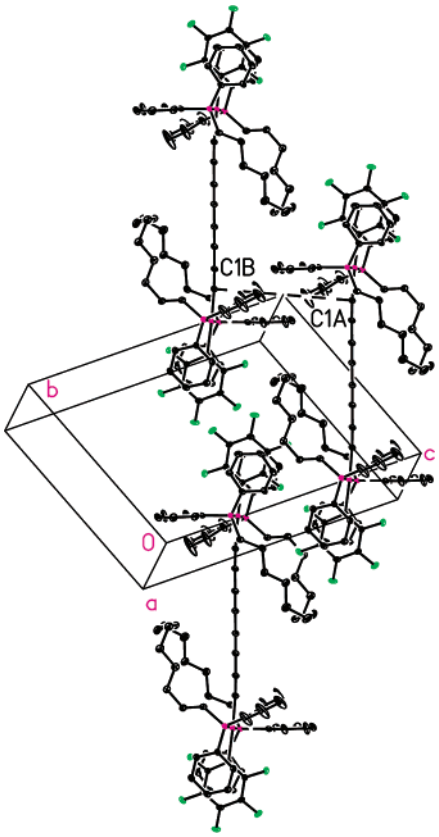

Figure 26. Packing diagram for C8-**24**·EtOH with solvent molecules omitted.

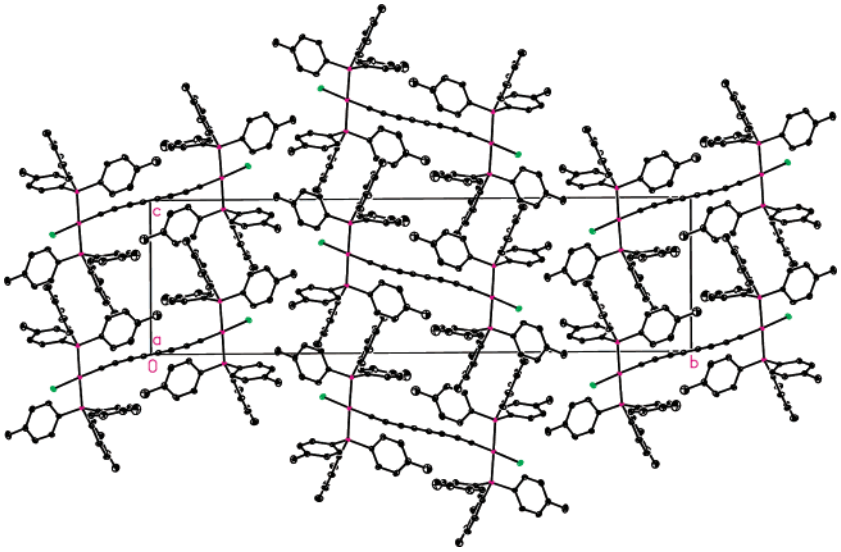

Figure 27. Packing diagram for C8-**25**·acetone.

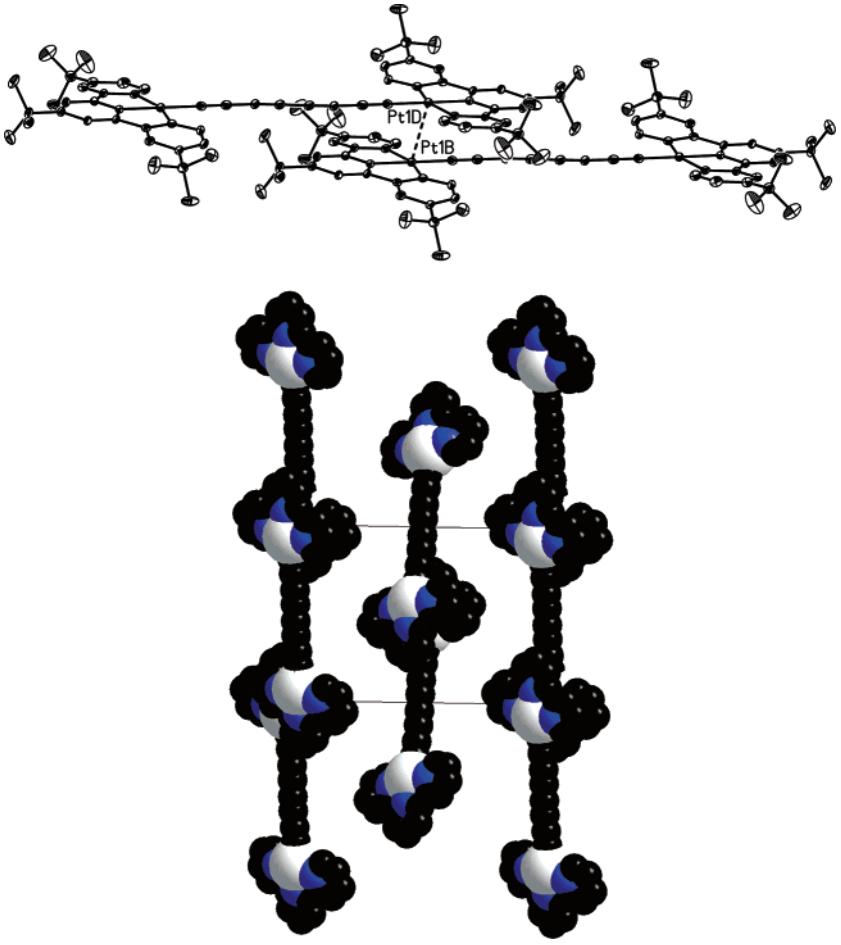

Figure 28. Packing diagram for C8-**27**·4acetone with solvent molecules and PF_6^- anions omitted (bottom: with *tert*-butyl groups omitted).

Consistent with observations above, the *p*-substituents on the arylphosphine ligands appear to play a role in the chain−chain spacing. The *p*-(*tert*-butyl) derivatives C8-**31**·5.5C_7H_8 and C8-**31**·2C_7H_8 exhibit the largest and third-largest distances between nearest parallel chains (11.985 and 11.433 Å). Figure 30 depicts the packing diagram of the former. The fractional offset values for the diplatinum complexes in Chart 4 show no regular trends. There is no obvious rationale for the very high offset of C8-**31**·2C_7H_8 (0.88), which corresponds to limit **P** in Figure 15, or the very low offset of C8-**32**·2$CHCl_3$ (0.10), which falls between limits **L** and **M**.

9.13. In terms of the remaining non-platinum-substituted tetraynes, some unique features of ditellurium compound C8-**10** deserve mention. This molecule crystallizes in the space group $P2/c$ ($Z = 4$) with two nonparallel sets of parallel chains as shown in

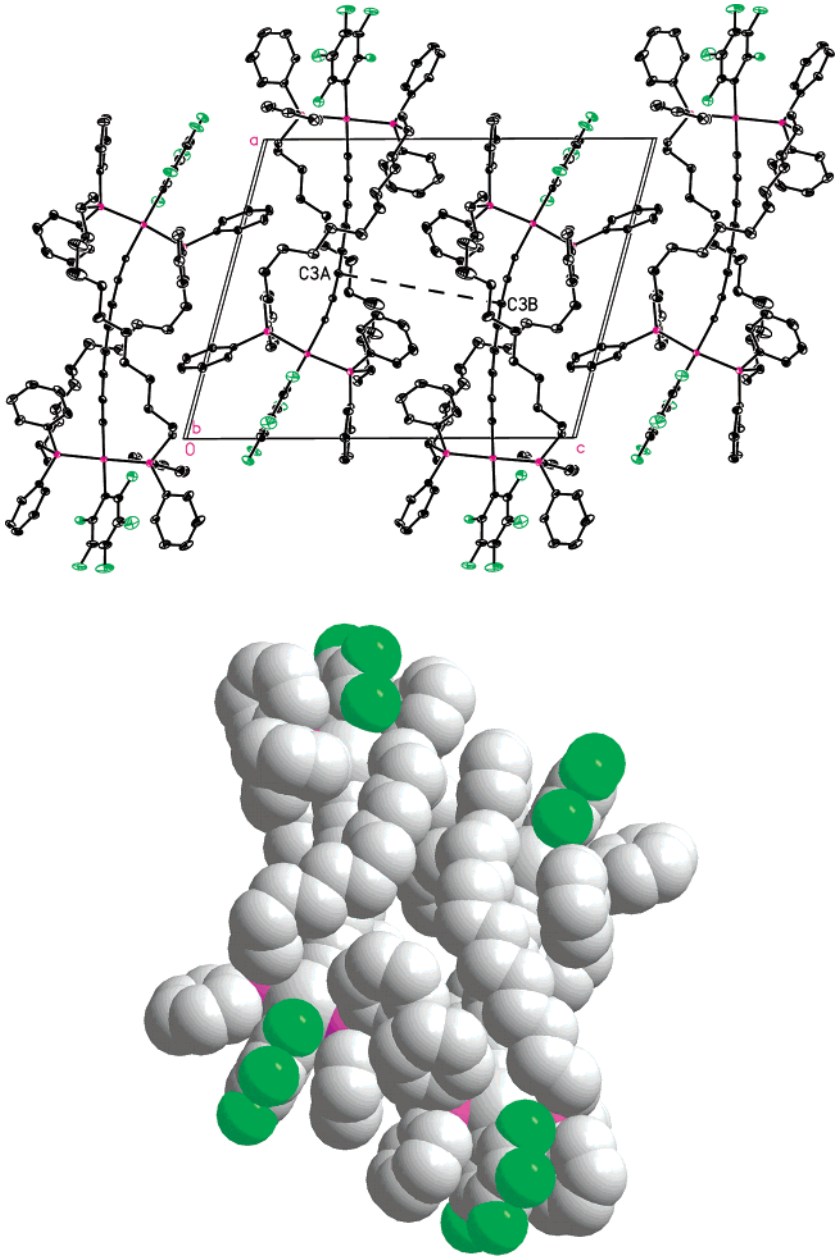

Figure 29. Packing diagram for C8-**29**·1.5C_6H_6 with solvent molecules omitted.

Figure 31. The closest parallel chains exhibit carbon−carbon (3.486 Å, C5A−C5F) and tellurium−tellurium (3.876 Å) contacts that are less than the sum of the van der Waals radii (4.4 Å for two tellurium atoms). The next-nearest parallel chains give very similar values (3.549 and 3.867 Å), and there are additional tellurium−tellurium contacts at 4.445 Å. The fractional offset, 0.08, is the second lowest in Table 5 (offset distance 1.02 Å). The torsion angle defined by the Te−CH_3 bonds (H_3C−Te···Te−CH_3) is 45.9(2)°, as easily visualized in the top perspective, but disguised in the bottom perspective. Also, the left and right horizontal stacks in the bottom perspective do not lie in the plane of the paper (the extreme left and right termini project away from the reader).

These peculiar geometric properties likely have a stereoelectronic origin. As noted by the authors,[30] the tellurium−carbon bonds in C8-**10** as well as crystallographically characterized lower homologues appear to be paired with tellurium 5p lone pair orbitals in neighboring molecules. The geometries, although not in C8-**10** collinear, are appropriate for lone pair/σ^* donor/acceptor interactions.[59] Hence, these compounds illustrate yet another type of intermolecular attraction that can play an important role in packing.

9.14. The hexaynes and octaynes in Charts 5−6 and Table 4 do, as noted above, show a trend toward lower offset angles Φ. However, the much longer "handle" in these dumbbell-like species does not lead to any fundamentally new packing motifs. For example, the diiron complex C12-**3** ($P2_1/c$, $Z = 4$), the chain conformation of which was analyzed above (Figure 13), crystallizes as depicted in Figure 32. This motif is similar to that of C8-**7a** in Figure 20. The closest distance between parallel chains (5.021 Å, C12D−C5E) is shorter than that between nonparallel chains (5.149 Å), and the fractional offset (0.42) is unremarkable. The other iron-containing hexayne, C12-**7**, crystallizes centrosymmetrically in $C2/m$ ($Z = 2$), and with all chains parallel. As noted above,

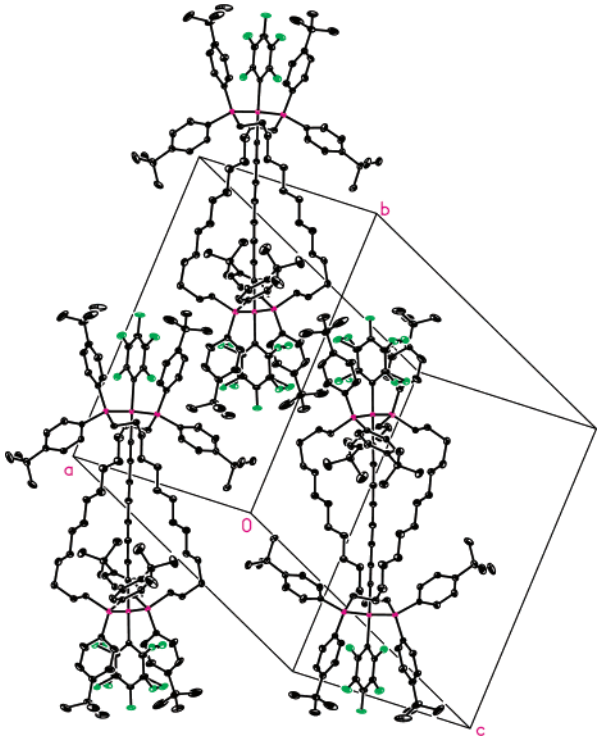

Figure 30. Packing diagram for C8-**29**·5.5C_7H_8 with solvent molecules omitted.

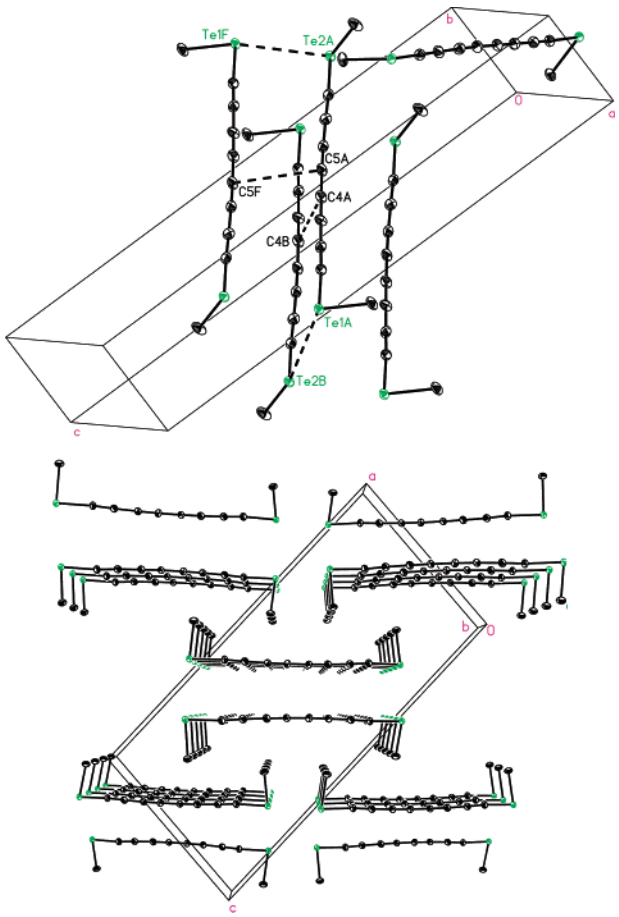

Figure 31. Packing diagram for C8-**10**.

the chains are essentially linear (ξ 0.01002). Accordingly, the closest chain−chain contact (3.512 Å) is the second-smallest after the ditellurium compound C8-**10**.

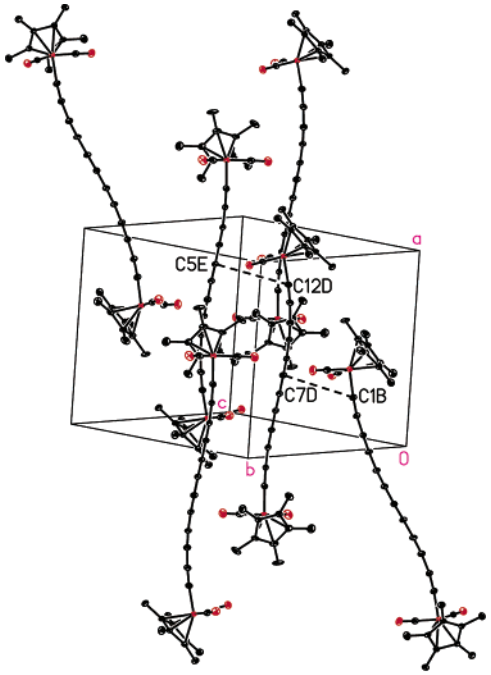

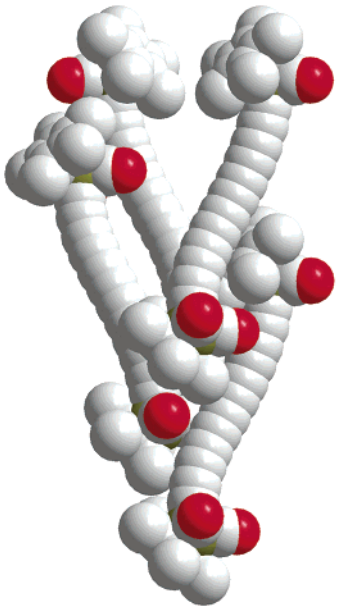

Figure 32. Packing diagram for C12-**3**.

The diplatinum hexayne C12-**4**·2C_6H_6 can be viewed as an extended version of tetraynes C8-**20**·4acetone·0.5$C_6H_4F_2$ or C8-**24**·EtOH, all of which crystallize in the same space group ($P\bar{1}$, $Z = 1$). The closest distance between parallel chains is somewhat less (7.884 vs 8.890−9.222 Å). The diplatinum hexayne C12-**5**·4C_6H_6·EtOH is (except for the solvate molecules) the exact higher homologue of tetrayne C8-**21**·C_7H_8. Interestingly, the space groups are identical ($P2_1/c$), although the Z value increases from 2 to 4. In the longer molecule, the closest distance between nearest parallel chains decreases considerably (7.884 vs 11.936 Å).

The diplatinum hexayne C12-**8** crystallizes centrosymmetrically in the space group C2 ($Z = 2$). All chains are parallel with a closest contact of 5.353 Å. This complex is the only one with *trialkyl*phosphine

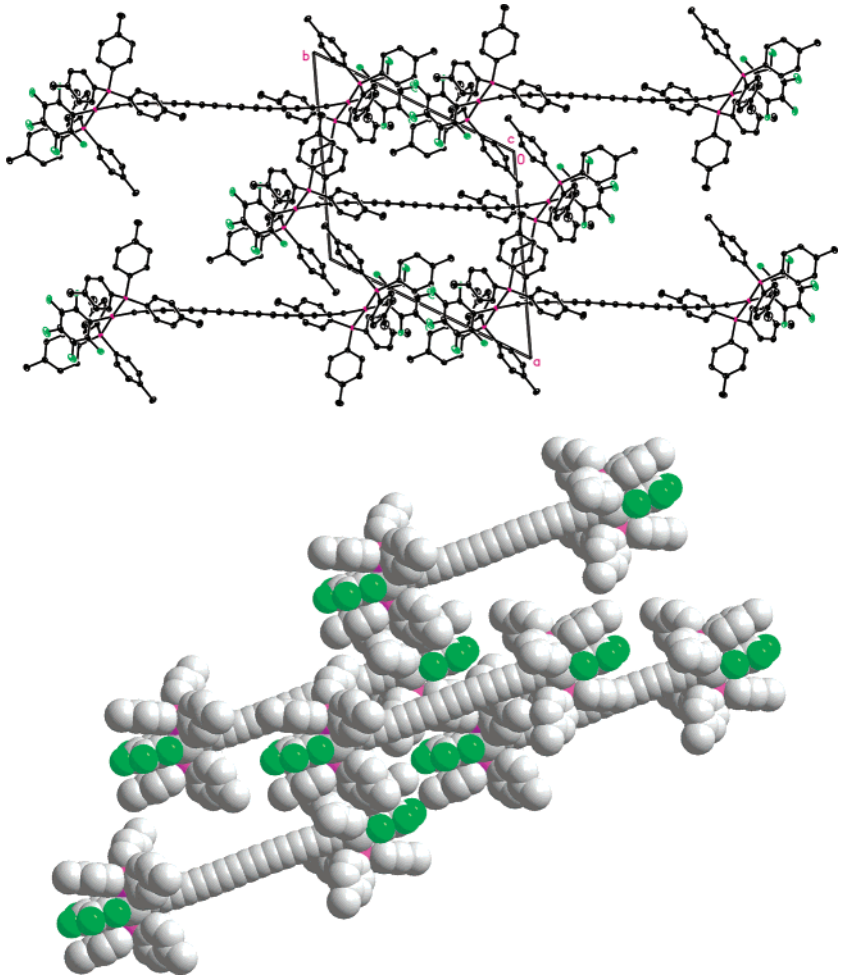

Figure 33. Packing diagram for C16-**1**·10C_6H_6 with solvent molecules omitted.

ligands. The more flexible ethyl groups may facilitate closer contacts as compared to more rigid aryl analogues. Finally, the diplatinum octayne C16-**1**·10C_6H_6 is (except for the solvate molecules) the exact higher homologue of C12-**5**·4C_6H_6·EtOH and C8-**21**·C_7H_8. Nonetheless, the space group changes to $P\bar{1}$ ($Z = 1$). Although the packing motif is quite similar to those of C8-**20**·4acetone·0.5$C_6H_4F_2$ or C8-**24**·EtOH (Figures 24 and 27), it is presented in Figure 33 to exemplify the longest structurally characterized polyyne to date.

9.15. Finally, two structurally similar tetraynes, C8-**2** and C8-**3**, display somewhat more complicated packing motifs that have no counterpart in the other polyynes. Both crystallize in identical orthorhombic space groups (*Pbcn*, $Z = 8$) with nearly the same unit cell dimensions. These feature *four* nonparallel sets of parallel chains, as distinguished by colors in the top view in Figure 34. One consequence is that it is not possible from any perspective to simultaneously display all chains in a fully elongated fashion (i.e., in the plane of the paper). The closest contacts between parallel chains are 3.853 and 4.018 Å. With C8-**2**, there is a closer contact with a nonparallel chain (3.593 Å).

10. Implications for Reactivity

The preceding data correlate in several ways to chemical properties. For example, simple acyclic alkynes such as 1- or 2-butyne have positive heats of formation, whereas analogous alkenes have negative heats of formation.[60] Polyynes have even more positive heats of formation. Accordingly, some higher polyynes—particular those with smaller endgroups such as hydrogen, halogen, or methyl—are known to be explosive.[61] In contrast, during 12 years of intensive efforts involving polyynes with transition metal endgroups, we have yet to encounter an explosion. It has been speculated that bulkier endgroups that enforce greater chain−chain separations give more stable compounds. Table 5 clearly shows that transition-metal endgroups give, on the average, larger solid-state chain−chain separations. It is certainly possible that other factors, such as the electropositive nature of transition-metal endgroups, also affect stabilities.

In a similar vein, topochemical polymerizations of crystalline 1,3-butadiynes to crystalline *trans*-polybutadiynes have been known for some time.[55] As illustrated in Figure 35 (top), these occur most readily when ϕ is ca. 45°, the distance between nearest parallel chains is ca. 3.5 Å, and the C1/C4 separation is 3.5−4.0 Å. This enables a close geometric match of the butadiyne and polybutadiyne crystal lattices, minimizing the change in the distance between the endgroups (5.1 Å). Recently, the first 1,6-topochemical polymerization of a 1,3,5-hexatriyne to a *trans*-polyhexatriyne was reported.[62,63] As shown in Figure 35 (middle), ϕ values of ca. 28° are optimal. Analo-

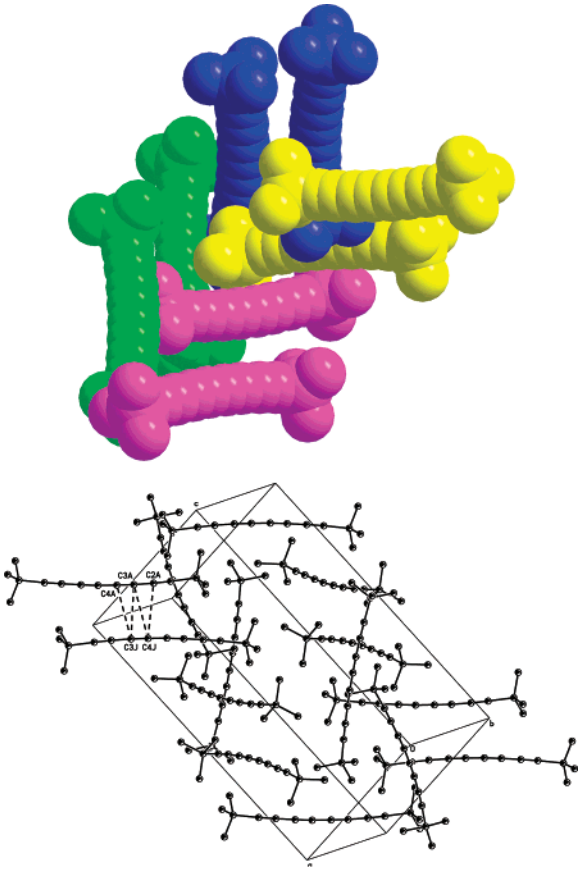

Figure 34. Packing diagram for C8-**2**.

gous polymerizations of 1,3,5,7-octatetraynes are not yet known, but ϕ values of ca. 21° would be required (Figure 35, bottom). In all of these cases, there is the obvious but sometimes overlooked additional requirement that the nearest neighbor contacts are not just for isolated pairs but propagate throughout the lattice.[64]

Subject to this caveat, the data in Table 5 can be used to screen candidates for such 1,4-, 1,6-, and 1,8-topochemical polymerizations. First, all lattices with chain−chain separations greater than 4.0 Å are eliminated. The centrosymmetric pentayne C10-**1**, with a ϕ value of 44.2° and a C1−C4 distance of 3.645 Å, stands out as an excellent candidate for a 1,4-polymerization. However, note that polymerization could equally well involve the C3/C6 carbons (distance 3.674 Å). The first mode would give C═C linkages with trans phenyl and -(C≡C)$_3$Ph groups, and the second trans -C≡CPh and -(C≡C)$_2$Ph groups. This polyyne, and all others highlighted below, stack with identical separations with appropriate symmetry for polymerization unless noted.[64]

The tetrayne C8-**7a**, with a ϕ value of 27.9° and a C1−C6 distance of 3.652 Å, would be one candidate for a 1,6-polymerization. Since this molecule is noncentrosymmetric, polymerization via C3−C8 coupling (distance 3.638 Å) would represent a distinct mode. In either event, the resulting polymer would be identical, with C═C linkages with trans X/C≡CX groups. The centrosymmetric tetrayne C8-**18**, with a ϕ value of 30.3° and C1−C6 and C3−C8 distances of 3.738 Å, would represent another possibility. The centrosymmetric hexayne C12-**7**, with a ϕ value of

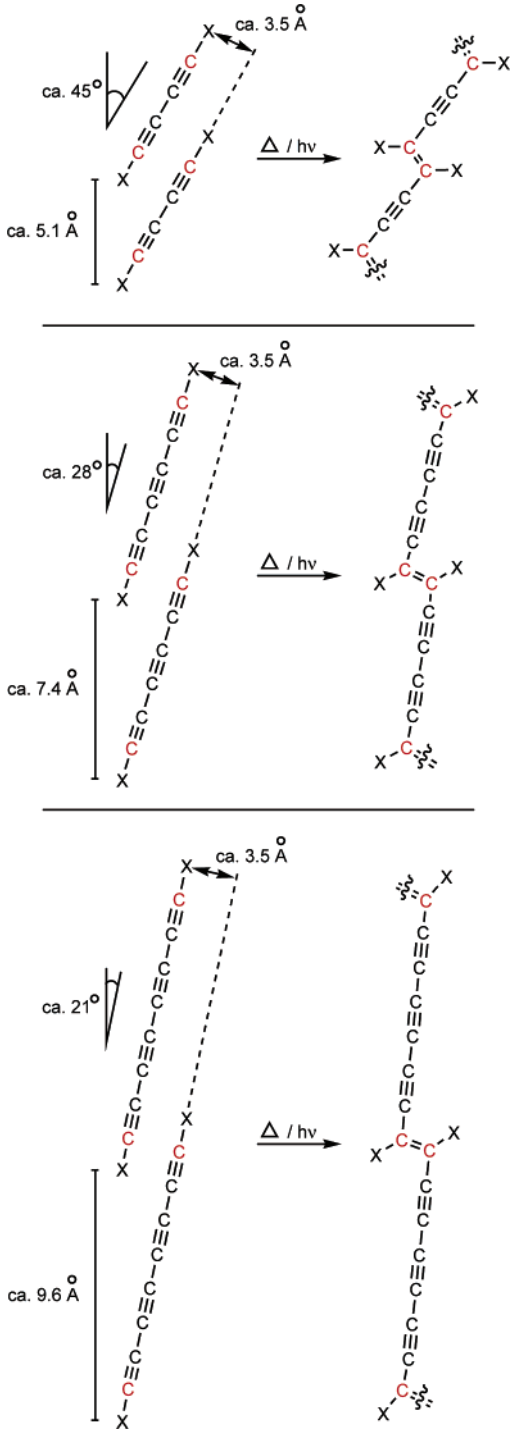

Figure 35. Topochemical polymerization of crystalline polyynes to crystalline *trans*-poly(polyynes).

29.3°, and C1−C6 and C3−C8 distances of 3.738 and 3.529 Å, is also a good candidate. A C1−C6 polymerization would give C═C linkages with trans ferrocenyl and -(C≡C)$_3$Fc groups, and a C3−C8 polymerization trans -C≡CFc and -(C≡C)$_2$Fc groups.

None of the polyynes in Table 5 crystallize in a manner ideal for a 1,8-topochemical polymerization. Compound C8-**27**·4acetone, with a ϕ value of 17.0° and a C1−C8 distance 6.110 Å, comes the closest. Clearly, it is just a matter of time before a good candidate is found. There appear to have been few attempts to polymerize crystalline samples of the above polyynes.[25] However, one solid-state polymer-

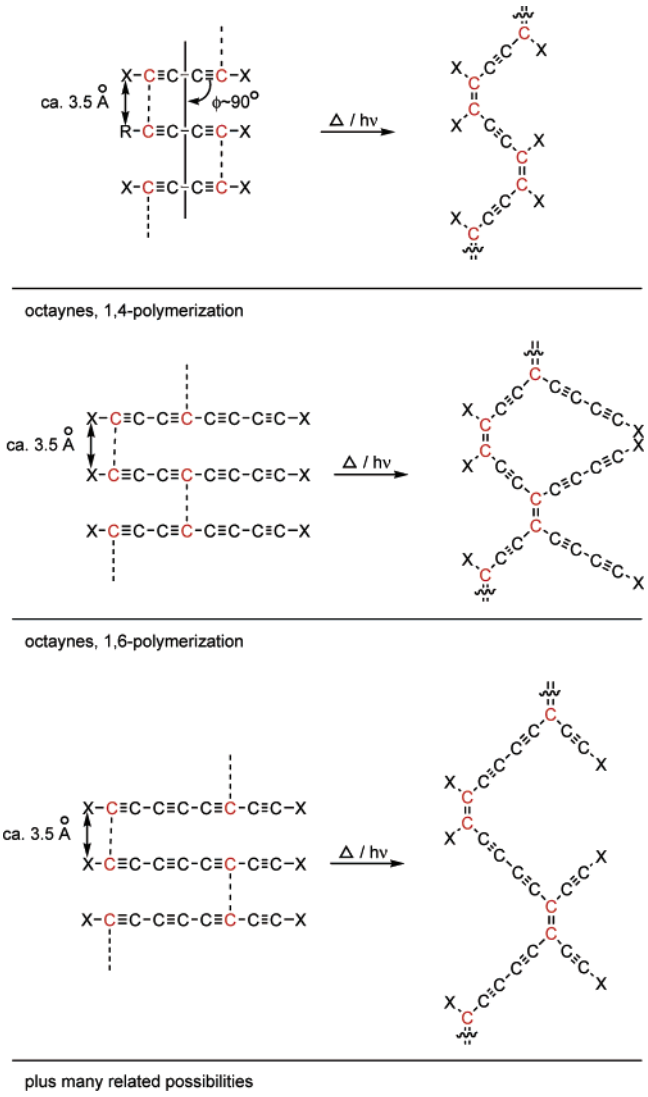

Figure 36. Polymerization of crystalline 1,3-butadiynes to *cis*-polybutadiynes, and representative extensions to higher polyynes.

ization of a hexayne characterized by powder X-ray diffraction has been reported.[65] Upon the basis of spectroscopic data, the authors propose that an initial 1,4-polymerization is followed by a 9,12-polymerization, yielding a network of dehydro[18]annulenes.

Other polymerization modes are possible for crystalline polyynes. For example, when 1,3-butadiynes are arrayed with a ϕ value of ca. 90° as in Figure 36, *cis*-polybutadiynes may be generated. Although such systems have been polymerized,[21] detailed product characterization remains in progress. In any event, C8-**8**, with a ϕ value of 83.9° and C1−C1 contacts of 3.924 Å, would represent one of the best candidates for this process. In principle, 1,4-1,6-, 1,8-, 3,6-, and other polymerization modes are possible, and the first two are illustrated in Figure 36. The ditellurium compound C8-**10**, with a ϕ value of 74.8° and many carbon−carbon contacts of ca. 3.6 Å, would at first appear to be another possibility. However, these contacts are not uniformly propagated throughout the lattice, and a true topochemical polymerization is impossible.[64]

Among the polyynes with poorer quality crystal structures that are not summarized in Tables 1−5, only one, C8-**5**, features parameters seemingly auspicious for polymerization. The ϕ value (49.4°) and C1−C4 or C3−C6 distances (3.799, 3.853 Å) would be appropriate for 1,4-topochemical polymerization as shown in Figure 35.[66] However, as with C8-**10**, the monomer packing pattern is not appropriate.[64] Indeed, efforts to effect polymerization were unsuccessful.[25] Finally, many polyynes with transition metal endgroups have very high decomposition points, often exceeding 250 °C.[4,5] These measurements are not generally performed on single crystals, which would often be complicated by desolvation. In some cases, IR evidence strongly implicates polymerization to give chain−chain cross-linked species.[4]

11. Summary and Conclusions

This review has summarized all currently available structural data for the title compounds. The major issues at the molecular level are bond lengths, bond angles, and sp carbon chain conformations. Averages derived from bond length or computational data suggest the following: (1) as the midpoints of the sp carbon chains are approached, the C−C bonds contract and the C≡C bonds lengthen; (2) as the chains are extended to the macromolecular limit of the one-dimensional carbon allotrope carbyne, the C−C bonds contract and the C≡C bonds lengthen. However, different asymptotic limits are approached, for which we propose values of 1.32−1.33 and 1.25 Å. Exceptions to (1) are evident in several molecules, and are likely due to endgroup effects. The error limits on the bond lengths (esd values) also preclude many comparisons. For this reason, computational chemistry will play an important role in the precise delineation of bond length trends.

The title compounds exhibit slightly lower bond angles near the end of the chain (X−C1−C2 < C1−C2−C3 < others). Nonetheless, pronounced bending remains possible throughout the chain, and six types of chain conformations have been defined (Figure 2). Strictly linear conformations (**A**) are never observed, although four molecules come quite close. Symmetric bow-shaped and S-shaped conformations (**B**, **E**) are quite common. Kinked and unsymmetric bow-shaped conformations (**D**, **C**) are also represented. In a few cases, secondary conformational features (e.g., spiraling) can be identified. Given the intrinsically low force constants and computed energies for *C*−*C*≡C or *X*−*C*≡C bending,[11,48,49] there is every reason to attribute the specific conformation observed to crystal packing effects. The deviation from linearity can be substantial, and one bow-shaped molecule (which is the most distorted by all criteria) can be regarded as having ca. 37% of the curvature of a semicircle. To best compare compounds with different conformations, a nonlinearity parameter (ξ) derived from a least-squares line has been defined.

Beyond the molecular level is the issue of lattice structure. Parallel chains are always evident. In some cases, all chains are parallel. In other cases, there are two or more sets of parallel chains with a nonparallel relationship. Our analysis has focused on the *closest* parallel chains. In a few molecules, contacts are very close to the sum of the sp carbon van der Waals radii (3.56 Å). Some of these are

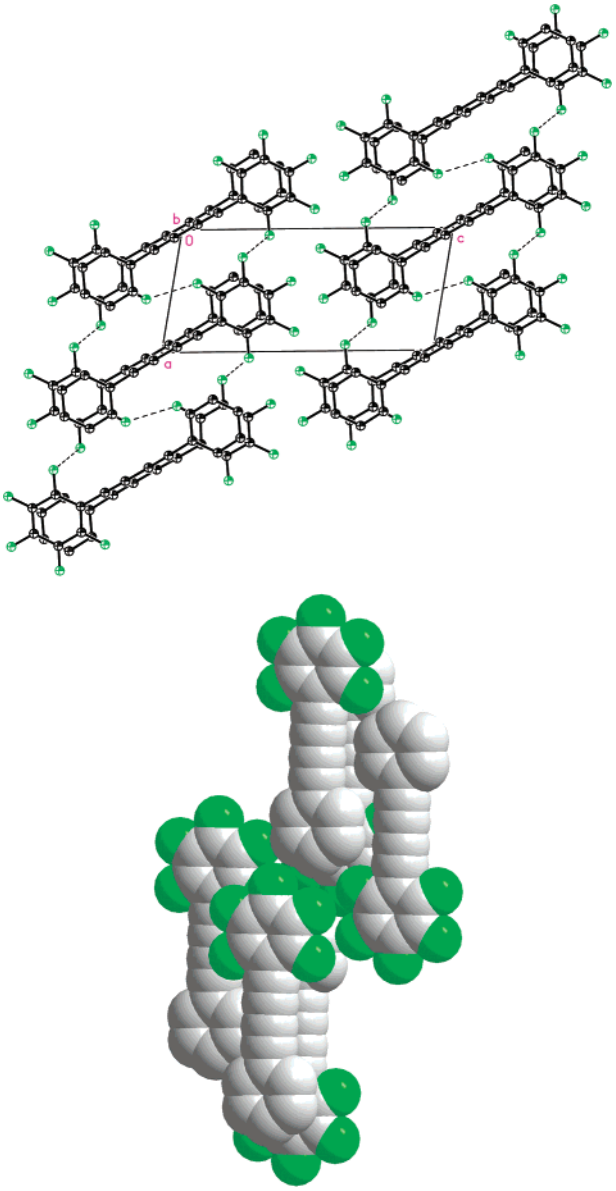

Figure 37. Packing diagram for the hemifluorinated diphenylbutadiyne $C_6H_5C{\equiv}CC{\equiv}CC_6F_5$.

promising candidates for topochemical polymerizations (Figures 35 and 36). The "translation" between closest parallel chains can be analyzed using various parameters, among which the "fractional offset" is most general (Figure 15). Values range from a low very close to zero (0.04, corresponding to simple vertical stacks of bricks) through 0.5 (traditional brick wall) to a high of 1.05. One might have expected, by analogy to physical objects such as dumbbells, that values close to 0.5 would be favored with bulky endgroups. However, no strong trend is apparent, although within certain series of compounds bulkier endgroups do lead to greater chain-chain separations.

Although additional fascinating features can be identified when individual crystal lattices are examined, there is little predictive capability at present regarding packing arrangements. Nonetheless, this compilation provides a very useful body of data for the future development of relationships. For example, how homologous will the crystal lattices of the series of diphenylpolyynes $Ph(C{\equiv}C)_nPh$ be? Are the effects of introducing *o*-bromo or *p*-(*tert*-butyl) substituents constant? Indeed, directed crystal engineering has already been achieved with lower polyynes. Diphenylbutadiyne $Ph(C{\equiv}C)_2Ph$ crystallizes without aryl/aryl stacking in a motif unsuitable for solid-state polymerization. However, the hemifluorinated analogue was found to crystallize with stacks of alternating C_6F_5 and C_6H_5 groups, as depicted in Figure 37.[21] The well-established quadrupolar attraction between such rings provides the driving force. This affords close C1−C1 contacts (3.68−3.73 Å; ϕ 81.5−72.3°), and polymerizations believed to be of the type in Figure 36 (top) could easily be effected.

It is obvious that there will be continued rapid growth of the number of higher polyynes in the literature, together with attendant crystallographic studies. As noted in the introduction, there were only seven crystallographically characterized tetraynes and pentaynes at the time of our first survey in 1997.[13] Since every new structure adds significantly to the present database, we plan regular updates in accord with a new "living review" format planned by this journal. Preprints of relevant work and/or private communications of unpublished structures are most welcome and will be incorporated with fitting acknowledgment.[67]

12. Acknowledgment

We thank the Deutsche Forschungsgemeinschaft (DFG; SFB 583) and Polish State Committee for Scientific Research (4 T09A 148 24) for support, and Professor R. Tykwinski (University of Alberta) for communicating unpublished data.

13. Supporting Information

Tabular data for lower-quality crystal structures. This material is available free of charge via the Internet at http://pubs.acs.org/cr.

14. References

(1) (a) Diederich, F.; Rubin, Y. *Angew. Chem.* **1992**, *104*, 1123; *Angew. Chem., Int. Ed. Engl.* **1992**, *31*, 1101. (b) Diederich, F. *Nature* **1994**, *369*, 199.
(2) (a) Curl, R. F. *Angew. Chem.* **1997**, *109*, 1636; *Angew. Chem., Int. Ed. Engl.* **1997**, *36*, 1567. (b) Kroto, H. *Angew. Chem.* **1997**, *109*, 1648; *Angew. Chem., Int. Ed. Engl.* **1997**, *36*, 1579. (c) Smalley, R. E. *Angew. Chem.* **1997**, *109*, 1666; *Angew. Chem., Int. Ed. Engl.* **1997**, *36*, 1595.
(3) Reviews and critical analyses: (a) Mel'nichenko, V. M.; Sladkov, A. M.; Nikulin, Yu. N. *Russ. Chem. Rev.* **1982**, *51*, 421. (b) Smith, P. P. K.; Buseck, P. R. *Science* **1982**, *216*, 984. (c) Kudryavtsev, Yu. P.; Heimann, R. B.; Evsyukov, S. E. *J. Mater. Sci.* **1996**, *31*, 5557. (d) Cataldo, F. *Polym. Int.* **1997**, *44*, 191. (e) Hlavaty, J.; Kavan, L.; Kasahar, N.; Oya, A. *Chem. Commun.* **2000**, 737.
(4) Compound C8-**16**: Dembinski, R.; Bartik, T.; Bartik, B.; Jaeger, M.; Gladysz, J. A. *J. Am. Chem. Soc.* **2000**, *122*, 810.
(5) Mohr, W.; Stahl, J.; Hampel, F.; Gladysz, J. A. *Chem. Eur. J.* **2003**, *9*, 3324.
(6) Schermann, G.; Grösser, T.; Hampel, F.; Hirsch, A. *Chem. Eur. J.* **1997**, *3*, 1105.
(7) Gibtner, T.; Hampel, F.; Gisselbrecht, J.-P.; Hirsch, A. *Chem. Eur. J.* **2002**, *8*, 408.
(8) Bildstein, B.; Schweiger, M.; Angleitner, H.; Kopacka, H.; Wurst, K.; Ongania, K.-H.; Fontani, M.; Zanello, P. *Organometallics* **1999**, *18*, 4286, and references therein.
(9) Compound C8-**3**: Lagow, R. J.; Kampa, J. J.; Wei, H.-C.; Battle, S. L.; Genge, J. W.; Laude, D. A.; Harper, C. J.; Bau, R.; Stevens, R. C.; Haw, J. F.; Munson, E. *Science* **1995**, *267*, 362.
(10) (a) Hunter, J. M.; Fye, J. L.; Roskamp, E. J.; Jarrold, M. F. *J. Phys. Chem.* **1994**, *98*, 1810. (b) Homan, K.-H. *Angew. Chem., Int. Ed.* **1998**, *37*, 2435.

(11) Lead references to bending frequencies: (a) Liang, C.; Allen, L. C. *J. Am. Chem. Soc.* **1991**, *113*, 1873. (b) Raghavachari, K.; Binkley, J. S. *J. Chem. Phys.* **1987**, *87*, 2191. (c) Roeges, N. P. G. *A Guide to the Complete Interpretation of Infrared Spectra of Organic Structures*; John Wiley & Sons: Chichester, 1994; p 226.

(12) Horný, L.; Petraco, N. D. K.; Pak, C.; Schaefer, H. F., III. *J. Am. Chem. Soc.* **2002**, *124*, 5861.

(13) Compound C8-**14**: Bartik, B.; Dembinski, R.; Bartik, T.; Arif, A. M.; Gladysz, J. A. *New J. Chem.* **1997**, *21*, 739.

(14) Compound C8-**1**: (a) Nitta, I. *Acta Crystallogr.* **1960**, *13*, 1035. (b) Watanabé, T.; Taguchi, I.; Masaki, N. *Acta Crystallogr.* **1959**, *12*, 347.

(15) Compound C8-**2**: Coles, B. F.; Hitchcock, P. B.; Walton, D. R. M. *J. Chem. Soc., Dalton* **1975**, 442.

(16) Compound C8-**13**: Altmann, M.; Enkelmann, V.; Bunz, U. H. F. *Chem. Ber.* **1996**, *129*, 269.

(17) Compound C8-**12**: Lin, J. T.; Wu, J. J.; Li, C.-S.; Wen, Y. S.; Lin, K.-J. *Organometallics* **1996**, *15*, 5028.

(18) Compound C10-**1**: Rubin, Y.; Lin, S. S.; Knobler, C. B.; Anthony, J.; Boldi, A. M.; Diederich, F. *J. Am. Chem. Soc.* **1991**, *113*, 6943.

(19) (a) Sharma, C. V. K. *Cryst. Growth Des.* **2002**, *2*, 465, and references therein. (b) Moulton, B.; Zaworotko, M. J. *Chem. Rev.* **2001**, *101*, 1629.

(20) Dunitz, J. *Chem. Commun.* **2003**, 545.

(21) Crystal engineering involving 1,3-butadiynes: Coates, G. W.; Dunn, A. R.; Henling, L. M.; Dougherty, D. A.; Grubbs, R. H. *Angew. Chem., Int. Ed. Engl.* **1997**, *36*, 248; *Angew. Chem.* **1997**, *109*, 290.

(22) Schwab, P. F. H.; Levin, M. D.; Michl, J. *Chem. Rev.* **1999**, *99*, 1863.

(23) (a) O'Keeffe, M.; Andersson, S. *Acta Crystallogr.* **1977**, *A33*, 914. (b) Flory, P. J.; Ronca, G. *Mol. Cryst. Liq. Cryst.* **1979**, *54*, 289.

(24) Compound C8-**4**: Sarkar, A.; Komatsu, K.; Okada, S.; Matsuda, H.; Nakanishi, H. *Acta Crystallogr.* **1998**, *C54*, 1519.

(25) Compound C8-**5**: Lee, L.-H.; Lynch, V.; Lagow, R. J. *J. Chem. Soc., Perkin Trans. 1* **2000**, 2805.

(26) Compound C8-**6**: Müller, T.; Hulliger, J.; Seichter, W.; Weber, E.; Weber, T.; Wübbenhorst, M. *Chem. Eur. J.* **2000**, *6*, 54.

(27) Compound C8-**7**: (a) Zhao, Y.; McDonald, R.; Tykwinski R. R. *Chem. Commun.* **2000**, 77. (b) Zhao, Y.; McDonald, R.; Tykwinski R. R. *J. Org. Chem.* **2000**, *67*, 2805.

(28) Compound C8-**8**: Heuft, M. A.; Collins, S. K.; Yap, G. P. A.; Fallis, A. G. *Org. Lett.* **2001**, *3*, 2883.

(29) Compounds C8-**9**, C8-**18**, C12-**1**: Tykwinski, R. R. and co-workers, unpublished data, University of Alberta.

(30) Compound C8-**10**: Werz, D. B.; Gleiter, R.; Rominger, F. *Organometallics* **2003**, *22*, 843.

(31) Compound C8-**15**: Dembinski, R.; Lis, T.; Szafert, S.; Mayne, C. L.; Bartik, T.; Gladysz, J. A. *J. Organomet. Chem.* **1999**, *578*, 229.

(32) Compound C8-**17**: Wong, K.-T.; Lehn, J.-M.; Peng, S.-M.; Lee, G.-H. *Chem. Commun.* **2000**, 2259.

(33) Compounds C8-**20**, C12-**4**: Peters, T. B.; Bohling, J. C.; Arif, A. M.; Gladysz, J. A. *Organometallics* **1999**, *18*, 3261.

(34) Compounds C8-**21**, C12-**5**, C12-**8**, C16-**1**: (a) Mohr, W.; Stahl, J.; Hampel, F.; Gladysz, J. A. *Inorg. Chem.* **2001**, *40*, 3263. (b) See also ref 5.

(35) Compound C8-**22**: Mohr, W.; Peters, T. B.; Bohling, J. C.; Hampel, F.; Arif, A. M.; Gladysz, J. A. *C. R. Chem.* **2002**, *5*, 111.

(36) Compounds C8-**23**-**26** and C10-**3**: Gladysz, J. A.; Hampel. F., and co-workers, unpublished results, Universität Erlangen-Nürnberg.

(37) Compound C8-**27**: Yam, V. W.-Y.; Wong, K. M.-C.; Zhu, N. *Angew. Chem., Int. Ed.* **2003**, *42*, 1400; *Angew. Chem.* **2003**, *115*, 1438.

(38) Compounds C8-**29**-**32**, C12-**9**: Stahl, J.; Bohling, J. C.; Bauer, E. B.; Peters, T. B.; Mohr, W.; Martín-Alvarez, J. M.; Hampel, F.; Gladysz, J. A. *Angew. Chem., Int. Ed.* **2002**, *41*, 1871; *Angew. Chem.* **2002**, *114*, 1951.

(39) Compound C12-**3**: Sakurai, A.; Akita, M.; Moro-oka, Y. *Organometallics* **1999**, *18*, 3241.

(40) Compound C12-**6**: Classen, J.; Gleiter, R.; Rominger, F. *Eur. J. Inorg. Chem.* **2002**, 2040.

(41) Compound C12-**7**: Adams, R. D.; Qu, B.; Smith, M. D. *Organometallics* **2002**, *21*, 3867.

(42) Threlfall, T. L. *Analyst* **1995**, *120*, 2435.

(43) (a) Fast, H.; Welsh, H. L. *J. Mol. Spectrosc.* **1972**, *41*, 1899. (b) McMullan, R. K.; Kvick, Å.; Popelier, P. *Acta Crystallogr.* **1992**, *B48*, 726.

(44) (a) Tanimoto, M.; Kuchitsu, K.; Morino, Y. *Bull. Chem. Soc. Jpn.* **1971**, *44*, 386. (b) Tay, R.; Metha, G. F.; Shanks, F.; McNaughton, D. *Struct. Chem.* **1995**, *6*, 47.

(45) March, J. *Advanced Organic Chemistry*; 4th ed.; Wiley: New York, 1992; pp 21−22.

(46) For average carbon−carbon bond lengths in crystallographically characterized molecules, see Allen, F. H.; Kennard, O.; Watson, D. G.; Brammer, L.; Orpen, G. A.; Taylor, R. *J. Chem. Soc., Perkin Trans. 2* **1987**, S1.

(47) (a) Zhuravlev, F.; Gladysz, J. A. Manuscript in preparation. (b) Jiao, H. Unpublished data, Universität Erlangen-Nürnberg.

(48) Green, D. C.; Englich, U.; Ruhlandt-Senge, K. *Angew. Chem., Int. Ed.* **1999**, *38*, 354; *Angew. Chem.* **1999**, *111*, 365.

(49) The angle given in ref 33 (19.7°) is incorrect.

(50) The assistance and input of Dr. J. Panek and Dr. K. Mierzwicki, University of Wroclaw, is gratefully acknowledged.

(51) Additional calibration tests were as follows. Semicircles with diameters or X−X′ distances of 9, 13, and 17 Å were constructed. Then 10, 14, and 18 atoms were spaced evenly along the circumference, corresponding to $X(C{\equiv}C)_nX'$ with n = 4, 6, 8 (resulting interatomic distances: 1.563, 1.567, 1.569 Å; % contractions: 56.3, 56.7, 56.9). The ξ values were 0.56657, 0.64343, and 0.71274, respectively. Next two semicircles were arranged in an S or ∩∪ shape, such that the termini or X−X′ distances were 9, 13, and 17 Å. Ten, 14, and 18 atoms were again spaced evenly along the circumference (resulting interatomic distances: 1.539, 1.555, 1.562 Å; % contractions: 53.9, 55.5, 56.2). The ξ values, 0.53009, 0.63718, and 0.72870, were similar to those of the single semicircles. Note that the least-squares lines for the single semicircles do not contain the endgroups, but those for the S-shaped double-semicircles must. Since the former can "float", it is intuitively plausible that the ξ values are approximately equal.

(52) (a) Gudipati, M. S.; Hamrock, S. J.; Balaji, V.; Michl, J. *J. Phys. Chem.* **1992**, *96*, 10165. (b) Levin, M. D.; Kaszynski, P.; Michl, J. *Chem. Rev.* **2000**, *100*, 169.

(53) Zorkii, P. M.; Oleinikov, P. N. *J. Struct. Chem.* **2001**, *42*, 24.

(54) Bondi, A. *J. Phys. Chem.* **1964**, *68*, 441.

(55) (a) Enkelmann, V. *Adv. Polymer Sci.* **1984**, *63*, 91. (b) Foley, J. L.; Li, L.; Sandman, D. J.; Vela, M. J.; Foxman, B. M.; Albro, R.; Eckhardt, C. J. *J. Am. Chem. Soc.* **1999**, *121*, 7262, and references therein. (c) Carré, F.; Devylder, N.; Dutremez, S. G.; Guérin, C.; Henner, B. J. L.; Jolivet, A.; Tomberli, V. *Organometallics* **2003**, *22*, 2014.

(56) Analogous calculations for all compounds in Table 5 were carried out using the midpoints of the carbon chains as opposed to the midpoints of the X/X′ vectors. In more than half the cases, the ϕ and offset values were identical. In a few cases, modest deviations were observed, corresponding to nonidealities resulting from the relative chain conformations (e.g., parallel and antiparallel relationships between molecules with bow conformations as discussed in the text).

(57) Desiraju, G. *Angew. Chem., Int. Ed. Engl.* **1995**, *34*, 2311; *Angew. Chem.* **1995**, *107*, 2541.

(58) Jennings, W. B.; Farrell, B. M.; Malone, J. F. *Acc. Chem. Res.* **2001**, *34*, 885.

(59) Gleiter, R.; Werz, D. B.; Rausch, B. J. *Chem. Eur. J.* **2003**, *9*, 2677.

(60) Benson, S. W. *Thermochemical Kinetics*; Wiley: New York, 1976.

(61) (a) Niedballa, U. In *Methoden der Organischen Chemie (Houben-Weyl)*, Müller, E., Ed.; Georg Thieme: Stuttgart, 1977; Vol V/2a, p 917. (b) Hunsmann, W. *Chem. Ber.* **1950**, *83*, 213. (c) See footnote 37 of ref 4.

(62) Xiao, J.; Yang, M.; Lauher, J. W.; Folwer, F. W. *Angew. Chem., Int. Ed.* **2000**, *39*, 2132; *Angew. Chem.* **2000**, *112*, 2216.

(63) See also Enkelmann, V. *Chem. Mater.* **1994**, *6*, 1337.

(64) It appears challenging to formulate the stacking requirement in terms of symmetry. When the polyyne occupies a special position (i.e., a 2-fold axis or symmetry center), polymerization will generally be possible, subject to the other metrical requirements. When the polyyne occupies a general position, the crystal lattice must be further scrutinized. When the nearest polyynes are related by a translation along any axis, a topochemical polymerization will be possible. Data for compounds analyzed: C10-**1**, special position, nearest neighbor relation: $x, y, z/x, 1+y, z$; C8-**7a**, general position, nearest neighbor relation: $x, y, z/x, 1+y, z$; C8-**18**, special position, nearest neighbor relation: $x, y, z/z, y-1, z$; C12-**7**, special position, nearest neighbor relation: x, y, z/x, y, $z-1$; C8-**27**·4acetone, special position, nearest neighbor relation: $x, y, z/x, 1+y, z$; C8-**8**, special position, nearest neighbor relation: $x, y, z/x-1, y, z$; C8-**10**, general position, nearest neighbor relation: $x, y, x/1-x, 2-y, 1-z$; C8-**5**, general position, nearest neighbor relation: $x, y, z/1-x, 1-y, 1-z$.

(65) Okada, S.; Hayamizu, K.; Matsuda, H.; Masaki, A.; Minami, N.; Nakanishi, H. *Macromolecules* **1994**, *27*, 6259.

(66) The value of ϕ that we calculate for C8-**5** (49.4°) differs from that reported (69°).[25]

(67) The following paper with new structural data appeared too late to include in the above analysis: Xu, G.-L.; Zou, G.; Ni, Y.-H.; DeRosa, M. C.; Crutchley, R. J.; Ren, T. *J. Am. Chem. Soc.* **2003**, *125*, 10057.

CR030041O